GROUND-BASED REMOTE SENSING OF THE BOUNDARY LAYER AND OFFSHORE WIND FARMS

Stefan Emeis
stefan.emeis@kit.edu

INSTITUTE OF METEOROLOGY AND CLIMATE RESEARCH, Atmospheric Environmental Research

Instruments:

surface-based (land, buoys, ships, …) scanning instruments

airborne platforms: aircraft, drones

Sites:

atmospheric boundary layers in flat and complex terrain,
(coastal) megacities, offshore wind farms

Topics:

internal boundary layers, boundary layer height, air quality,
land-sea wind systems, low-level jets, wind resources

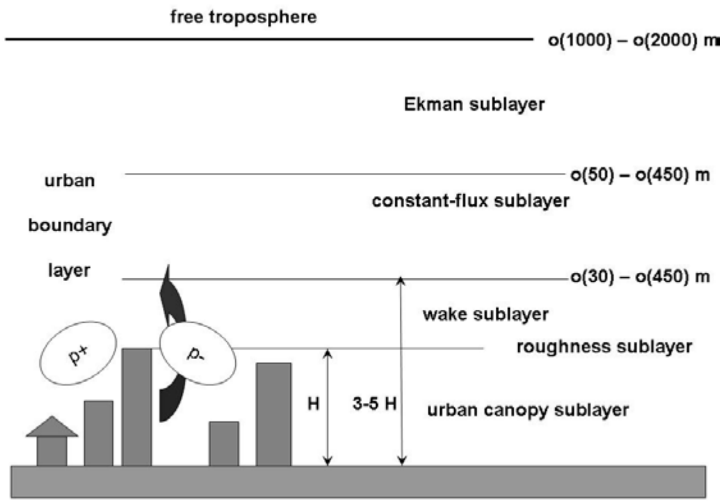

urban BL

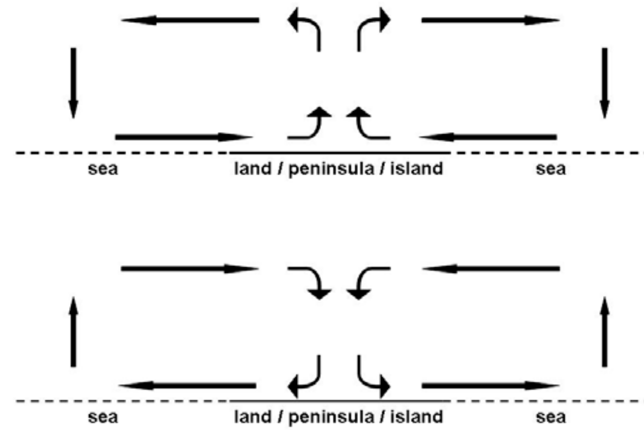

thermally induced secondary circulations

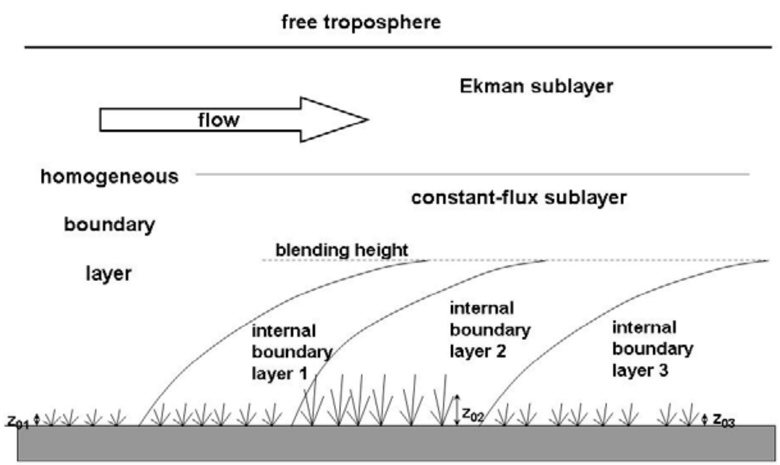

internal BLs

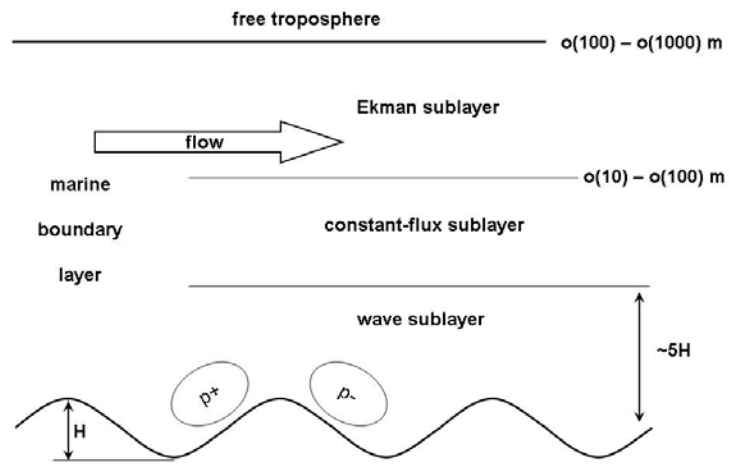

marine BL

Photo: 2011 Stefan Emeis

Warmer cities influence local and regional climate (Clouds over Manhattan on May 28, 2011)

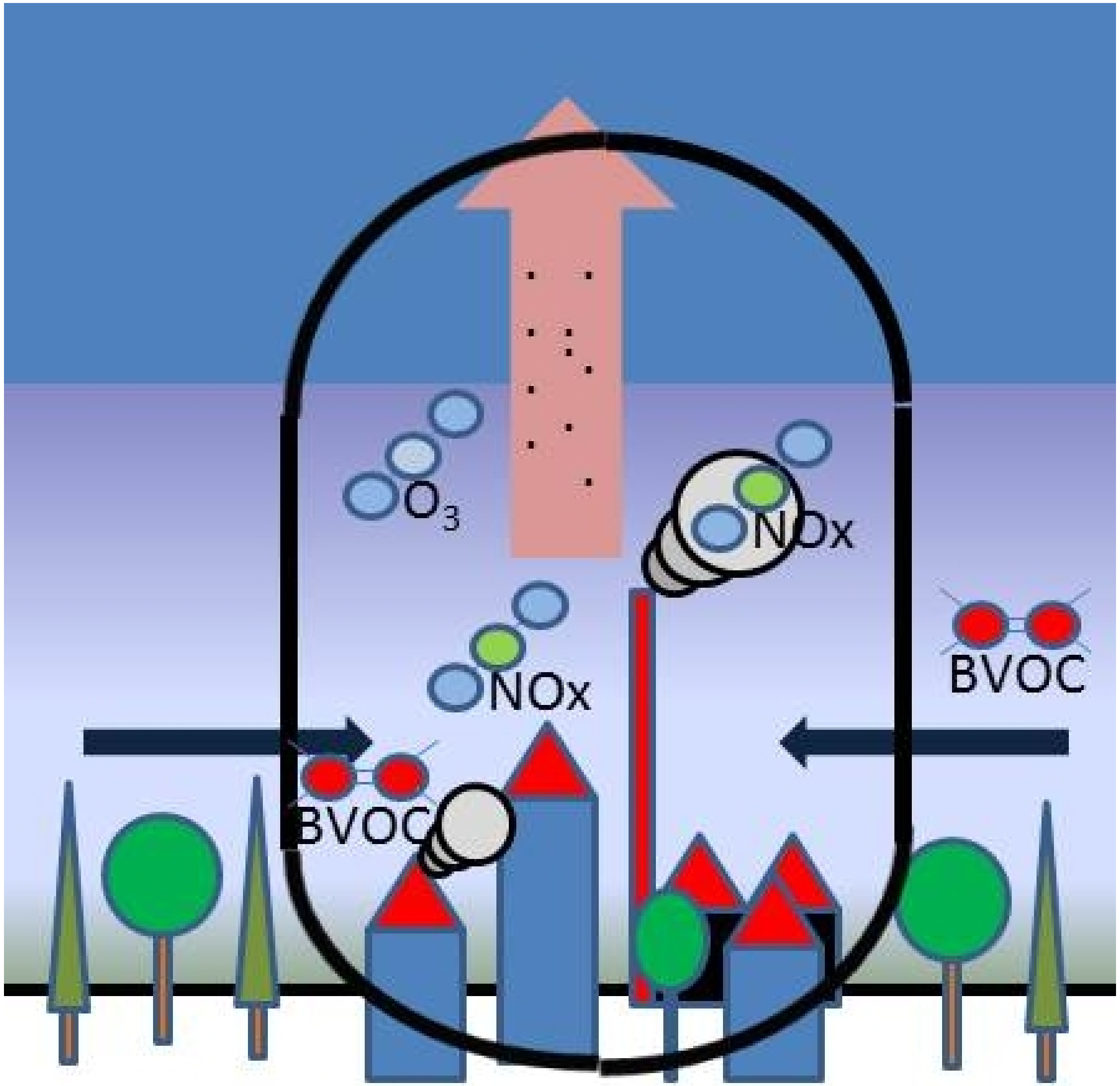
O3
NOx
NOx
BVOC
BVOC

Swedish offshore farm Lillgrund
(Öresund) 110.4 MW
48 turbines (2.3 MW)

Coastal farm near Rødby
(Denmark)

Erected and planned offshore wind farms in the North Sea

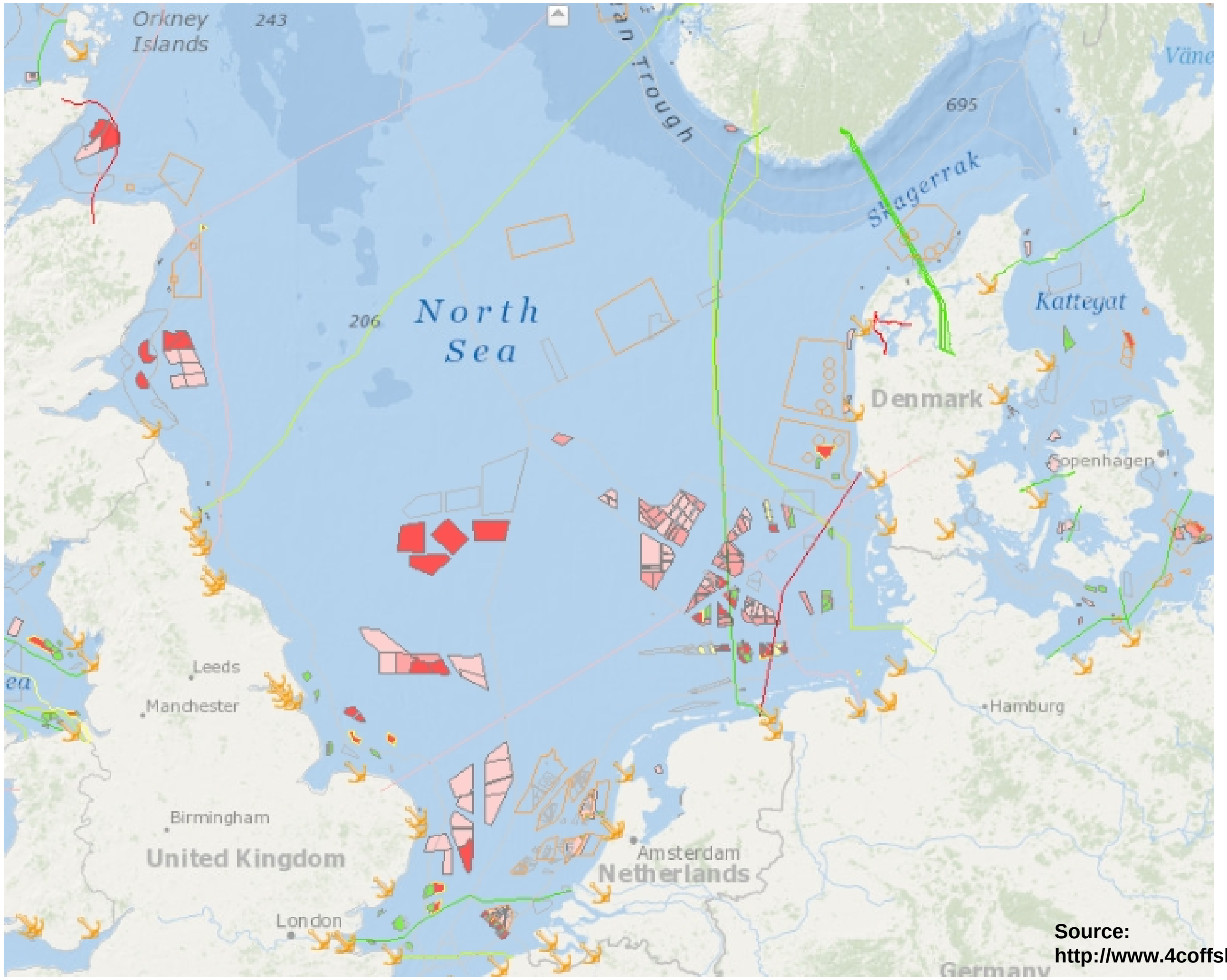

Source:
http://www.4coffshore.com/offshorewind/

Measurement techniques

in situ

temperature
humidity
wind (speed, direction, turbulence)
pressure
radiation (UV, SW, LW, sunshine)
cloudiness
precipitation (rain, snow, hail)
visibility
atmospheric electricity

air quality (gases, aerosols)
radioactivity

sea surface temperature
waves (height, speed, direction)

remote sensing

temperature
humidity (?)
wind (speed, direction, turbulence)

optical depth
ceiling, cloud-top temperatures
precipitation
optical backscatter intensity

air quality (gases, aerosols)

sea surface temperature
waves (height, speed, direction)

Platforms	Characteristics/variables	Types of measurement
underground	soil temperature, soil moisture,	continuous, in-situ
surface	surface properties, surface fluxes,	continuous, in-situ, remote sensing
shelter or screen	2 m height, near-surface air properties,	continuous, in-situ
(street) cars	near-surface properties	continuous, along route
buoy	near-surface characteristics	continuous, in-situ, remote sensing
ship, oil rig	some meters above the sea,	in-situ along seaways
mast	up to some hundred meters,	continuous, in-situ, profile
unmanned aerial vehicle (UAV)	up to several hundreds of metres	in-situ along flight path
ultralight aircraft	up to several kilometres	in situ along flight path
tethered balloon	up to several hundred meters,	sequential profile measurements
constant-level balloon	floats in a given height,	in-situ along flight path
radiosonde	up to 30 km height,	single profile measurement
aircraft	flexible flight track,	in-situ+remote along flight path
satellite	only remote sensing	remote sensing, path-averaged, sounding

Remote sensing of the atmosphere

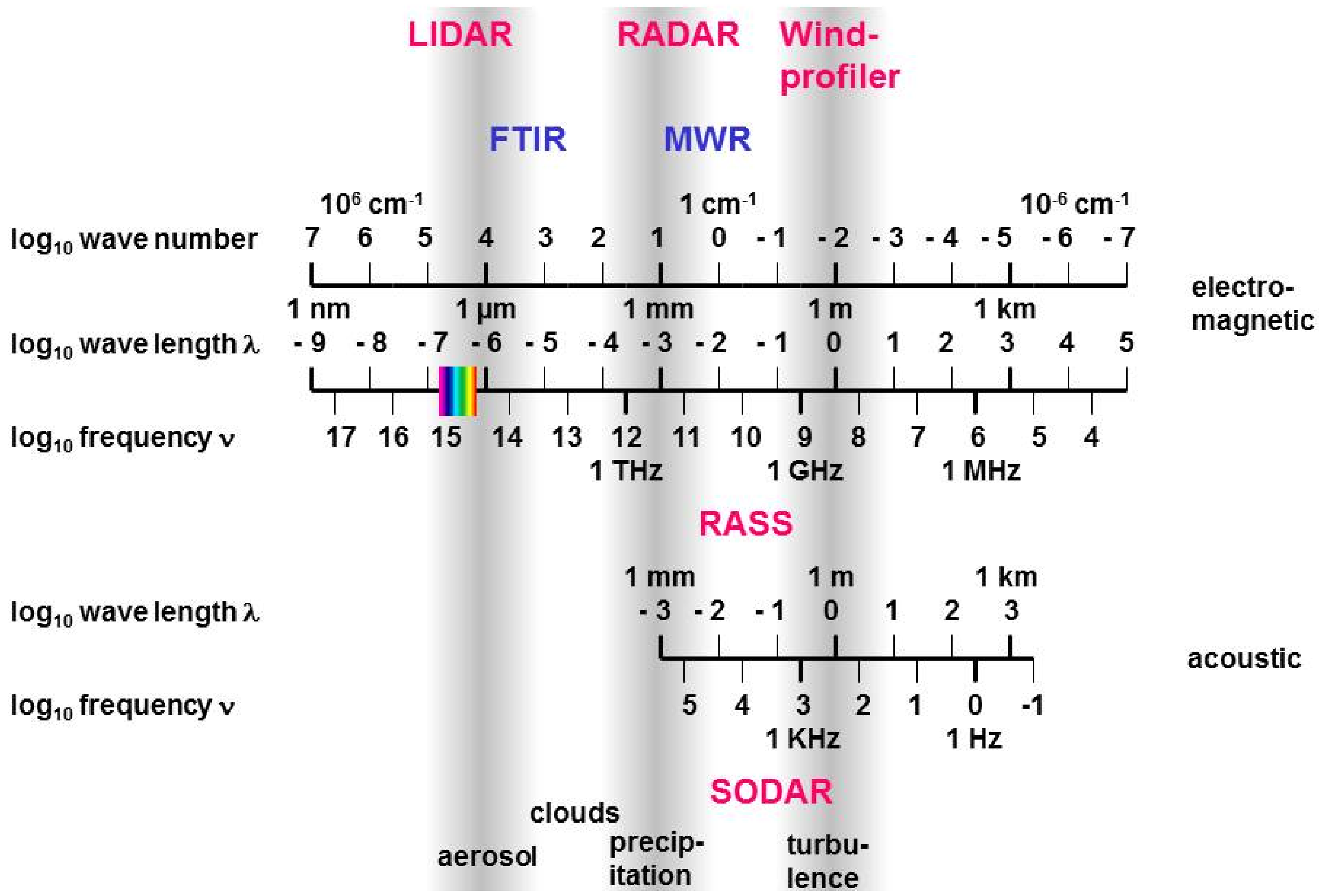

SODAR

algorithms for the determination of mixing-layer height

and low-level jet observations

SODAR, acoustic backscatter, Doppler shift analysis ➔ wind, turbulence

three antennas

phased-array

Basic principle of a phased-array sodar

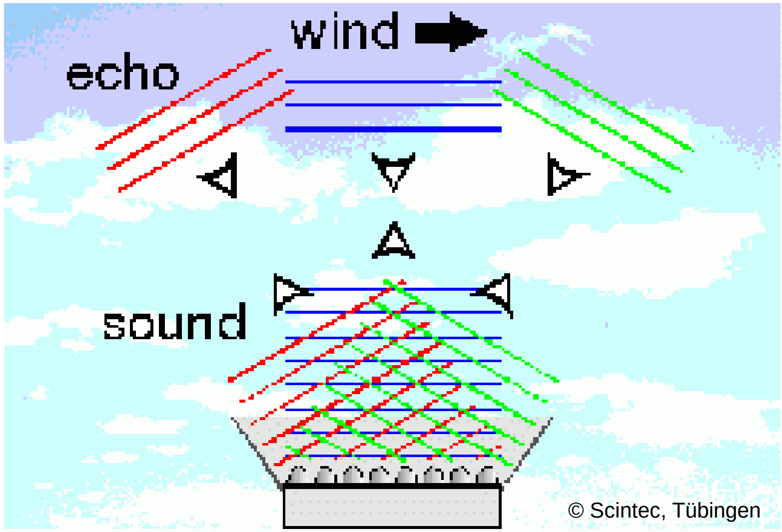

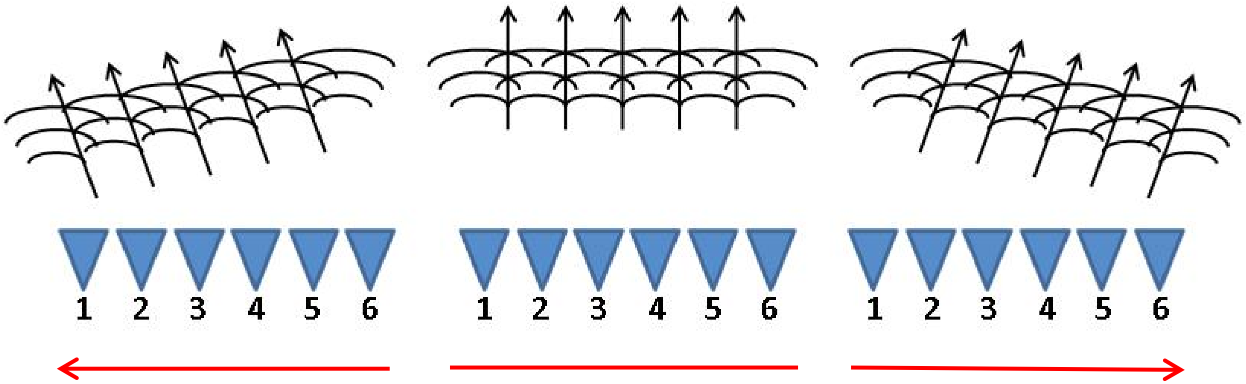

monostatic SODAR: measuring principles

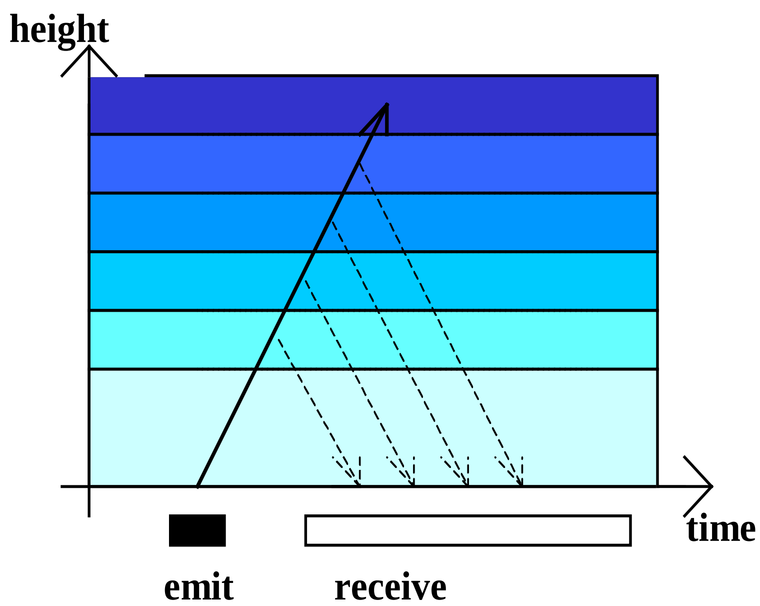

deduction:

sound travel time	=	height
backscatter intensity	=	turbulence
Doppler-shift	=	wind speed

The SODAR equation:

$$P_R = r^{-2} \left(c_s \tau A \varepsilon / 2\right) P_0 \, \beta_s \, e^{-2\sigma r} + P_{bg}$$

P_R received power,
P_0 emitted power,
ε antenna efficiency,
A effective antenna area,
σ sound absorption in air due to classical and molecular absorption due to the collision of water molecules with the oxygen and nitrogen molecules of the air,
r distance between the scattering volume and the instrument,
τ pulse duration (typically between 20 and 100 ms),
β_s backscattering cross-section (typically in the order of 10^{-11} m^{-1} sr^{-1}),
c_s sound speed,
P_{bg} background noise.

Emitted power: ~ 10^3 W, received (backscattered) power: 10^{-15} W

SODAR sample plot (daytime convective BL)

acoustic backscatter intensity

40 – 300 m

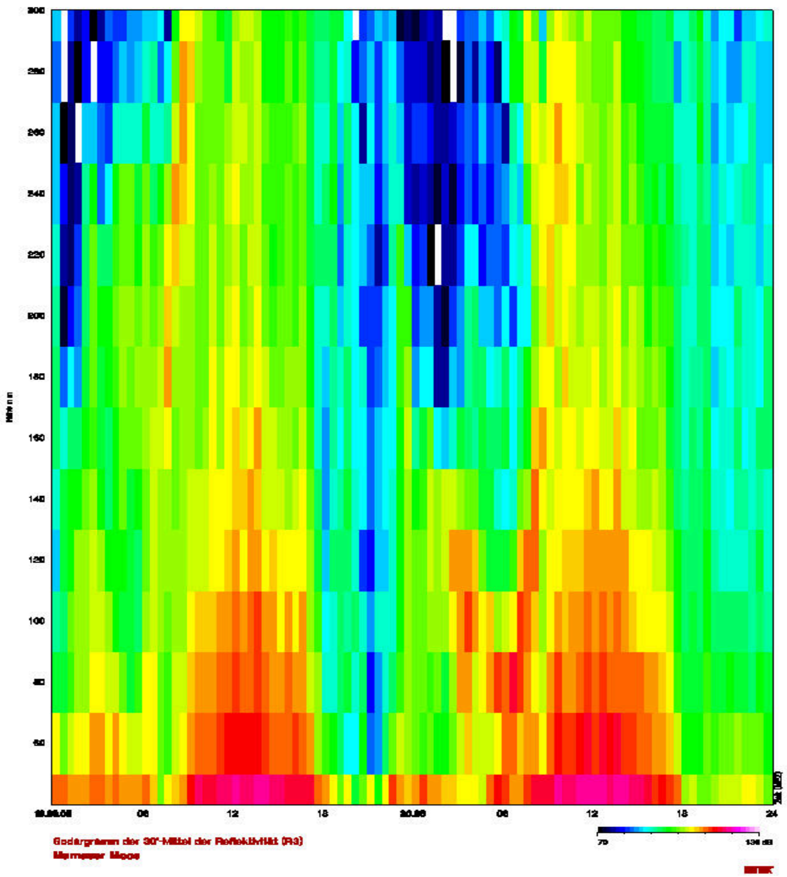

2 days, midnight to midnight

sigma w

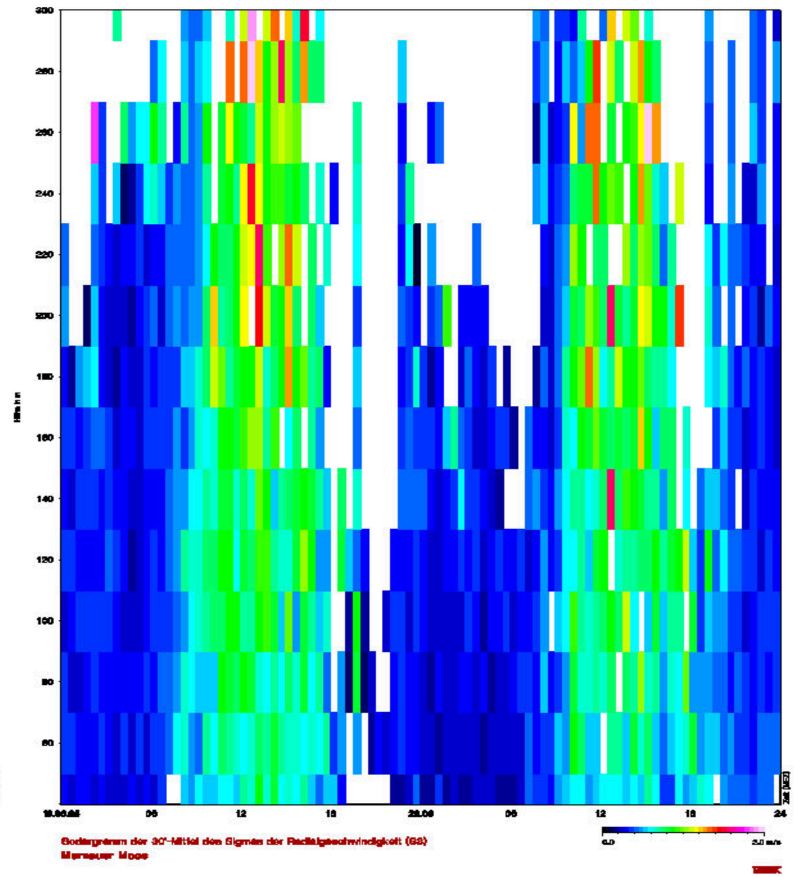

Institute for Meteorology and Climate Research – Atmospheric Environmental Research

SODAR sample plot (lifted inversion)

acoustic backscatter intensity

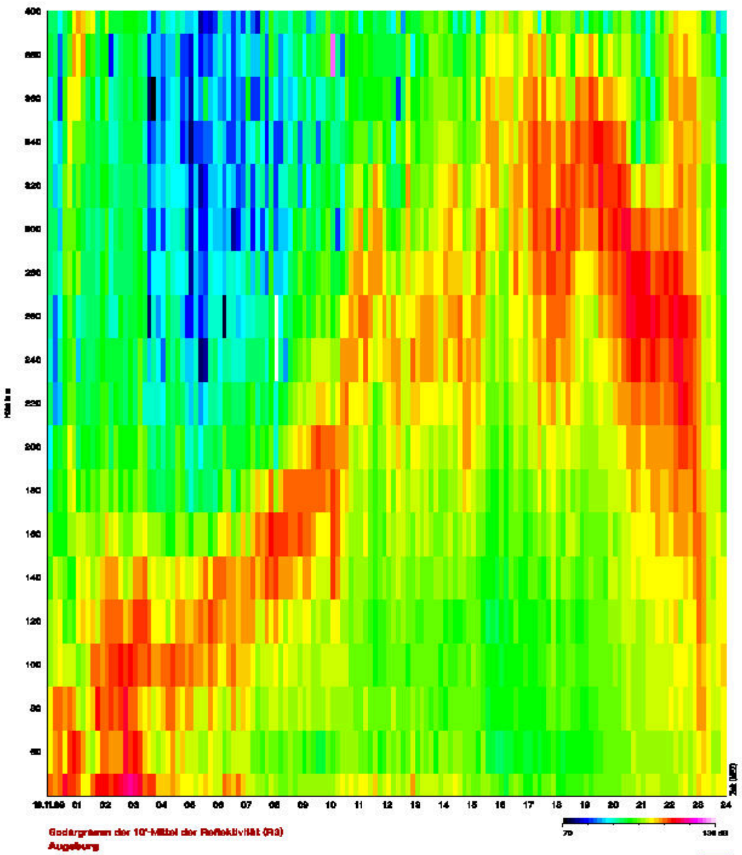

sigma w

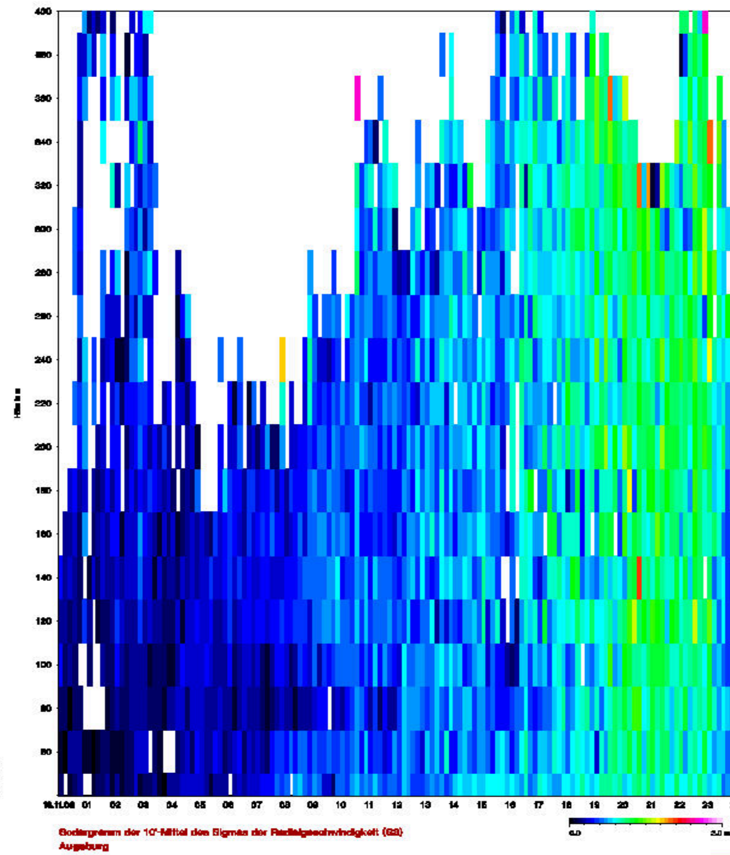

40 – 400 m

1 day, midnight to midnight

Algorithms to detect MLH from SODAR data

criterion 1:
upper edge of high turbulence

criterion 2:
surface and lifted inversions

MLH = Min (C1, C2)

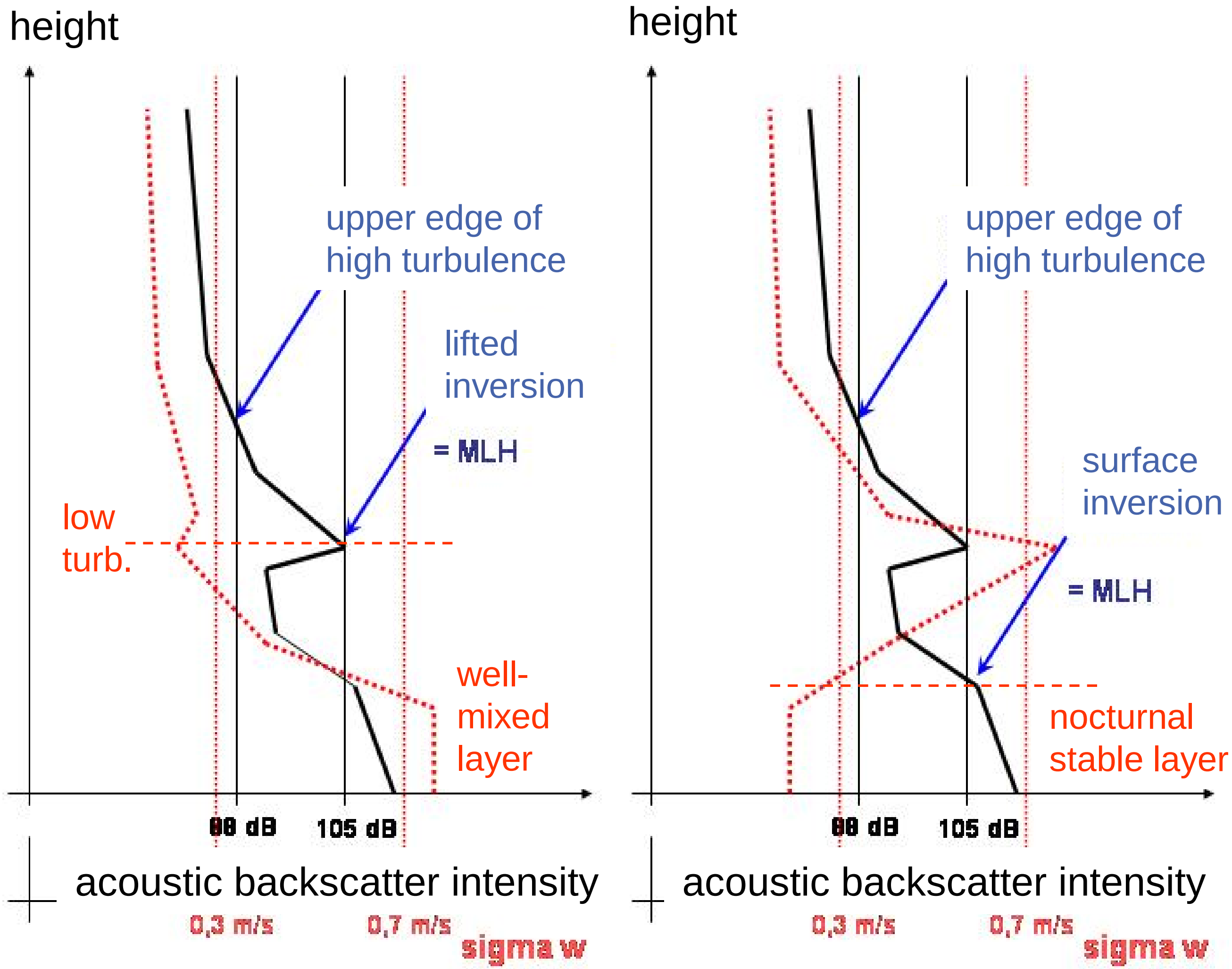

example 1: daytime

example 2: night-time

Emeis, S., K. Schäfer, C. Münkel, 2008: Surface-based remote sensing of the mixing-layer height – a review. Meteorol. Z., **17**, 621-630.

Ceilometer

algorithms for the determination of mixing-layer height

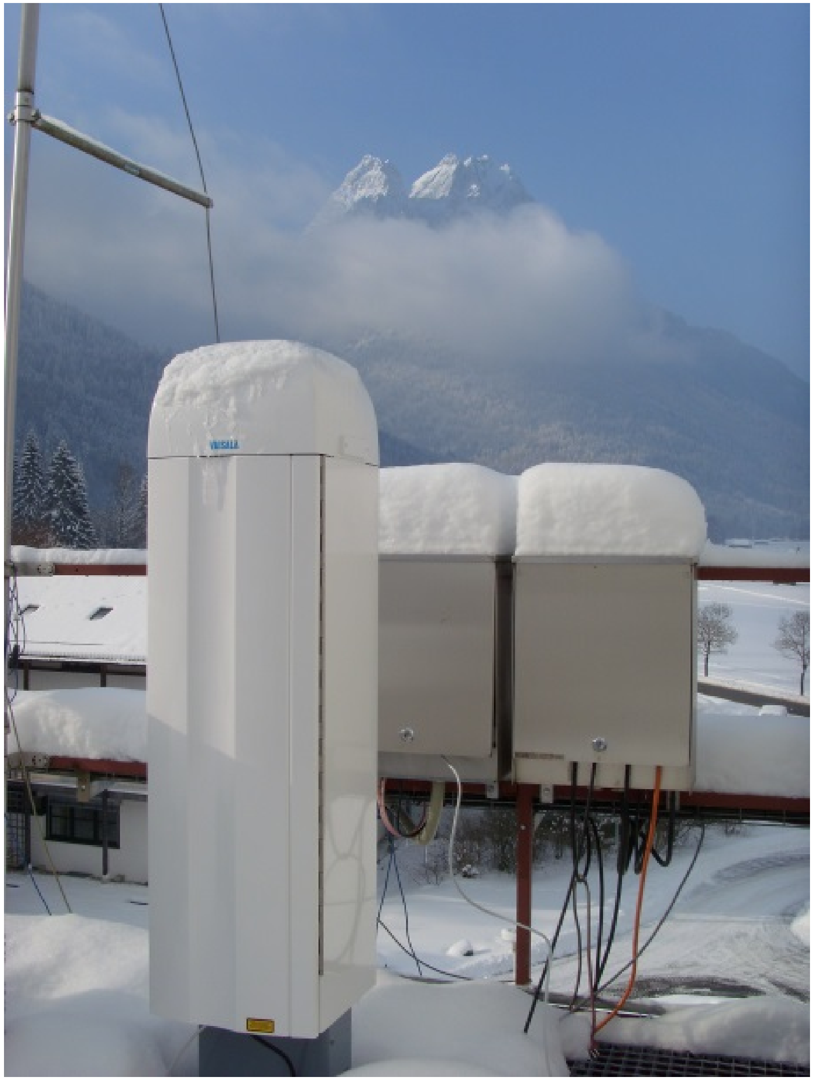

Ceilometer, optical backscatter,
pulsed emission,
wave length ~ 0.9 µm

➔ aerosol profiles

Ceilometer/LIDAR measuring principle

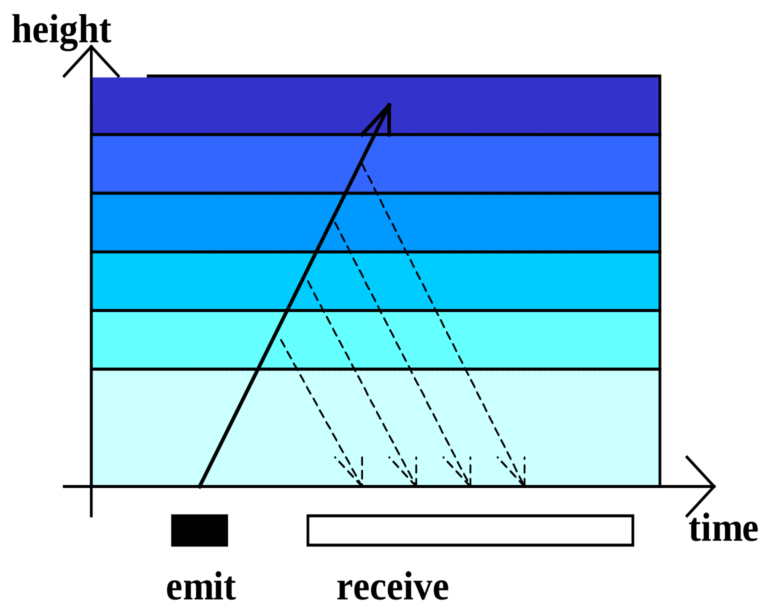

detection:

travel time of signal = height
backscatter intensity = particle size and number distribution
Doppler-shift = cannot be analyzed from ceilometer data
(available only from a Wind-LIDAR: velocity component in line of sight)

The LIDAR equation:

$$P_R(\lambda,r) = r^{-2}\,(c\tau A\varepsilon/2)\,P_0\,[\beta_m(\lambda,r) + \beta_p(\lambda,r)]\,e^{-2\sigma r} + P_{bg}$$

r distance between the LIDAR and the backscattering object,
c speed of light,
τ pulse duration,
A antenna area,
ε correction term for the detector efficiency and losses due to the lenses,
P_0 emitted energy,
β_m backscatter coefficient for molecules
β_p backscatter coefficient for particles,
σ absorption of light in the atmosphere,
P_{bg} background noise.

For a ceilometer β_m is negligible and only β_p is important

ceilometer sample plot (daytime convective BL)

optical backscatter intensity

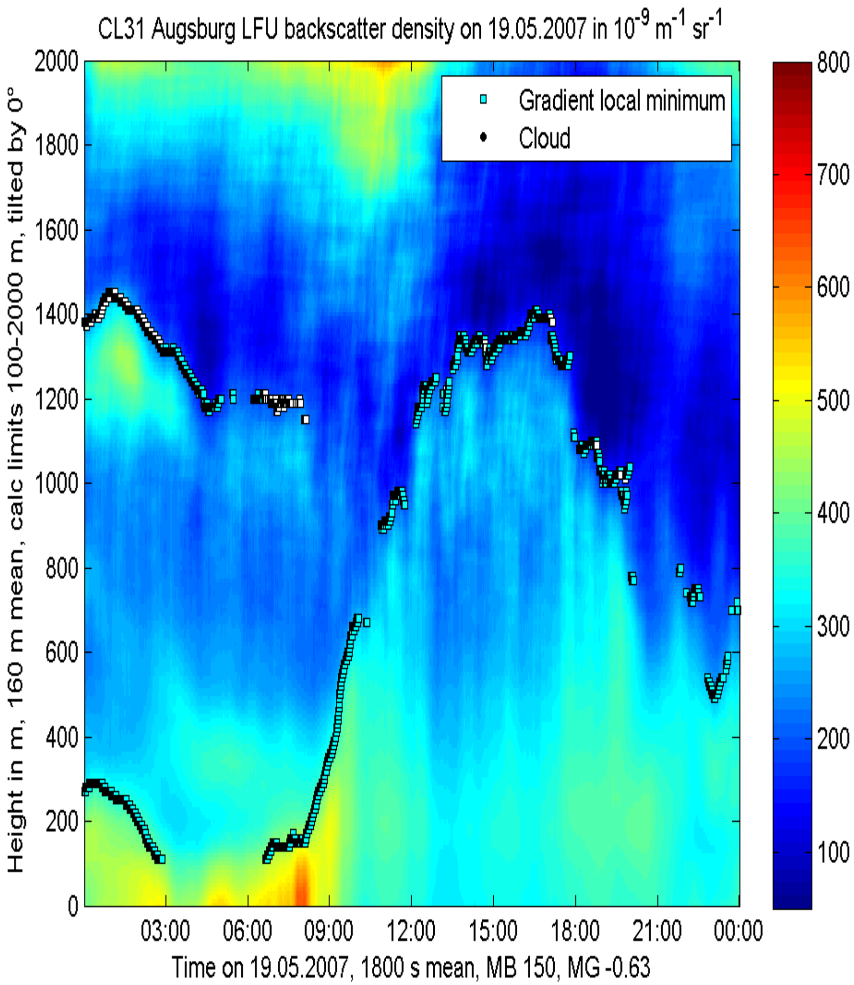

negative vertical gradient of optical backscatter intensity

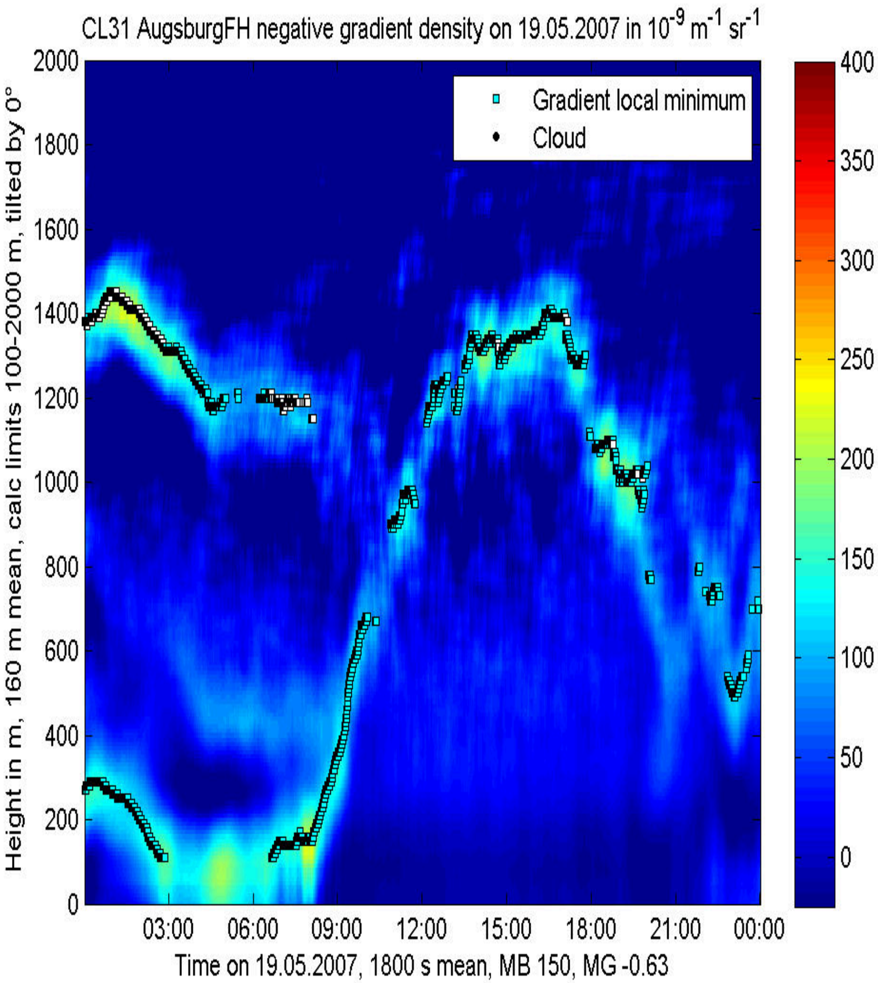

Institute for Meteorology and Climate Research – Atmospheric Environmental Research

Algorithm to detect MLH from Ceilometer-Daten

criterion

minimal vertical gradient of backscatter intensity (the most negative gradient)

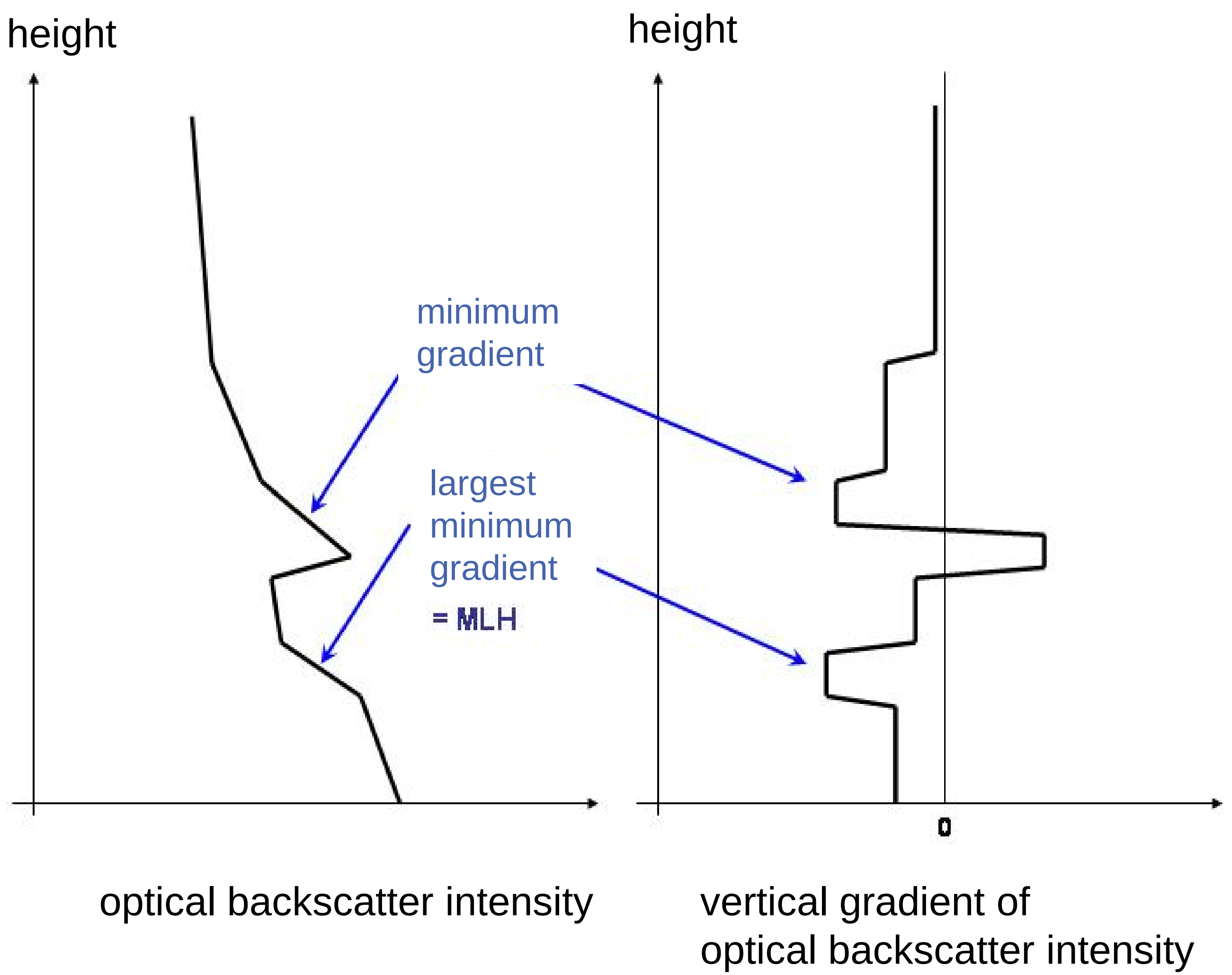

Different gradient methods (see Sicard et al. 2006, BLM 119, 135-157)

logarithmic gradient minimum

gradient minimum

inflection point method
(minimum of 2nd derivative)

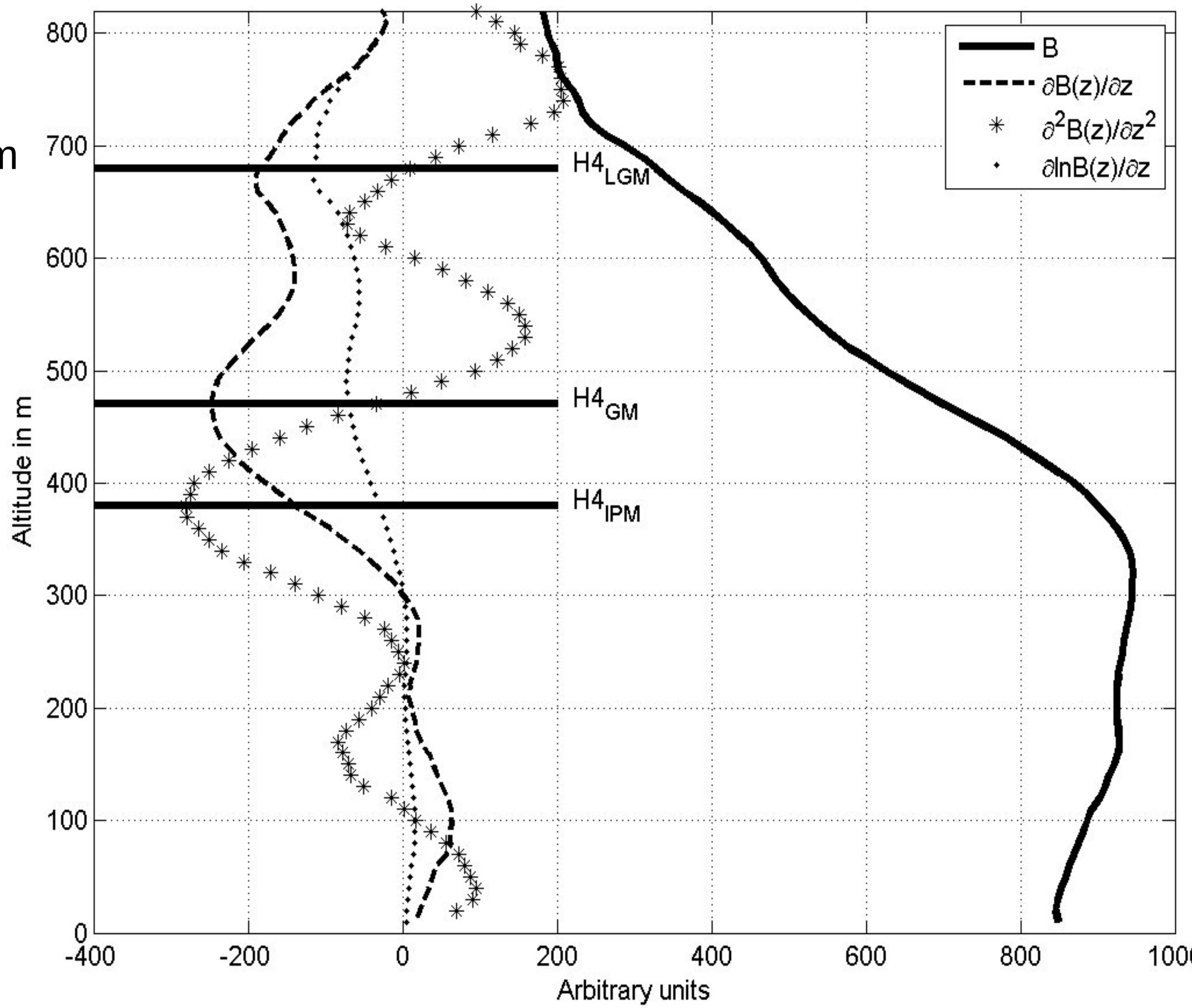

Institute for Meteorology and Climate Research –
Atmospheric Environmental Research

comparison of two different ceilometers

LD40

two optical axes
- wave length: 855 nm
- height resolution: 7.5 m
- max. range: 13000 m

CL31 / CL51

one optical axis
- wave length: 905 nm
- height resolution: 5 m
- max. range: 7500 m

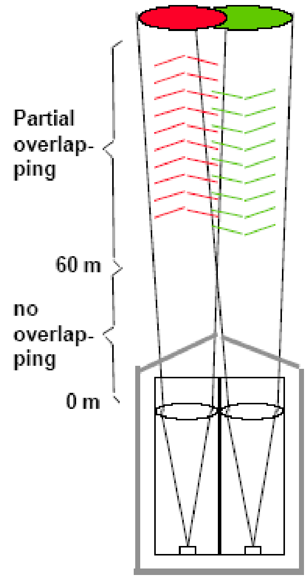

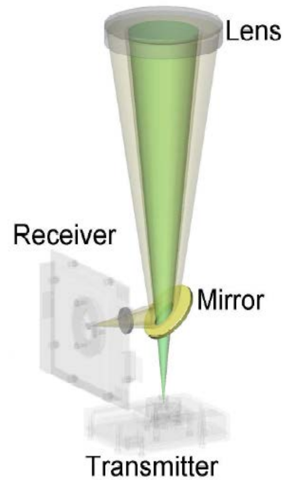

comparison of LD40 and CL31

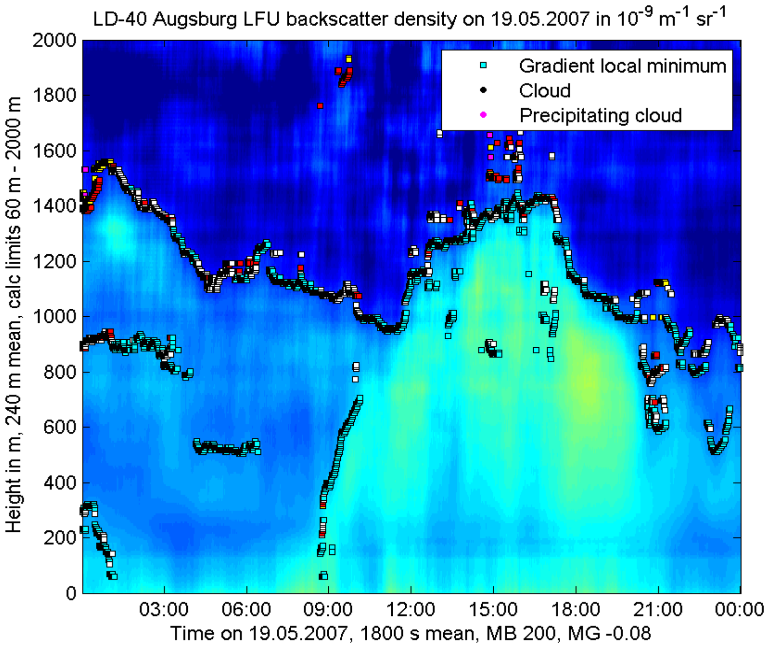

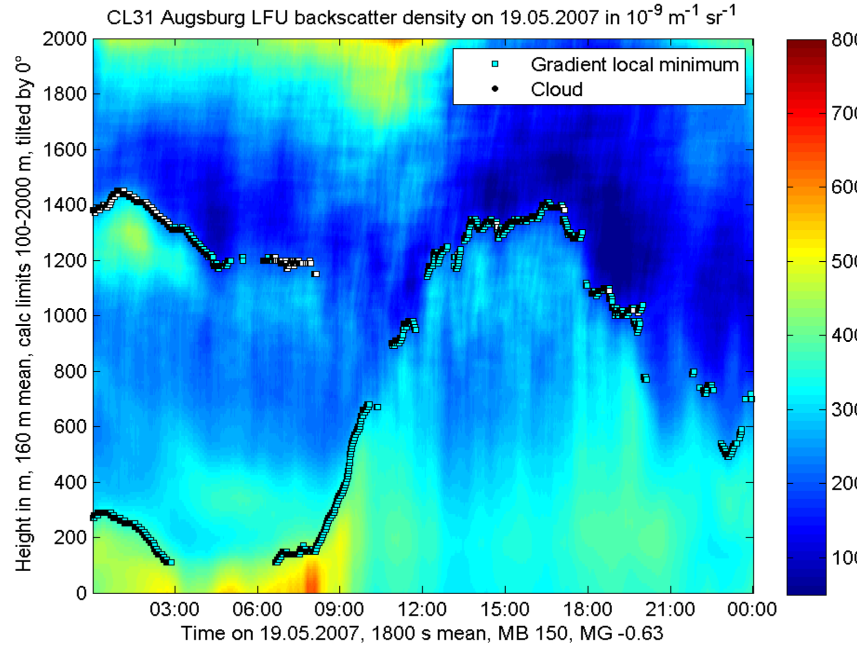

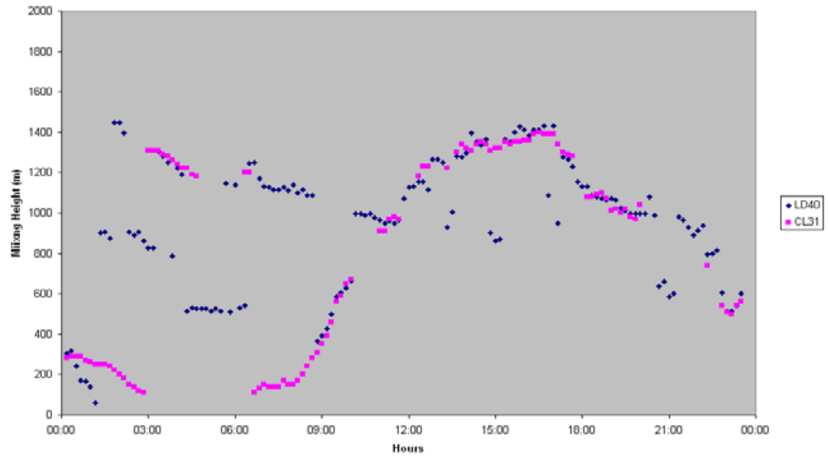

Eyjafjallajökull ash cloud over Southern Germany

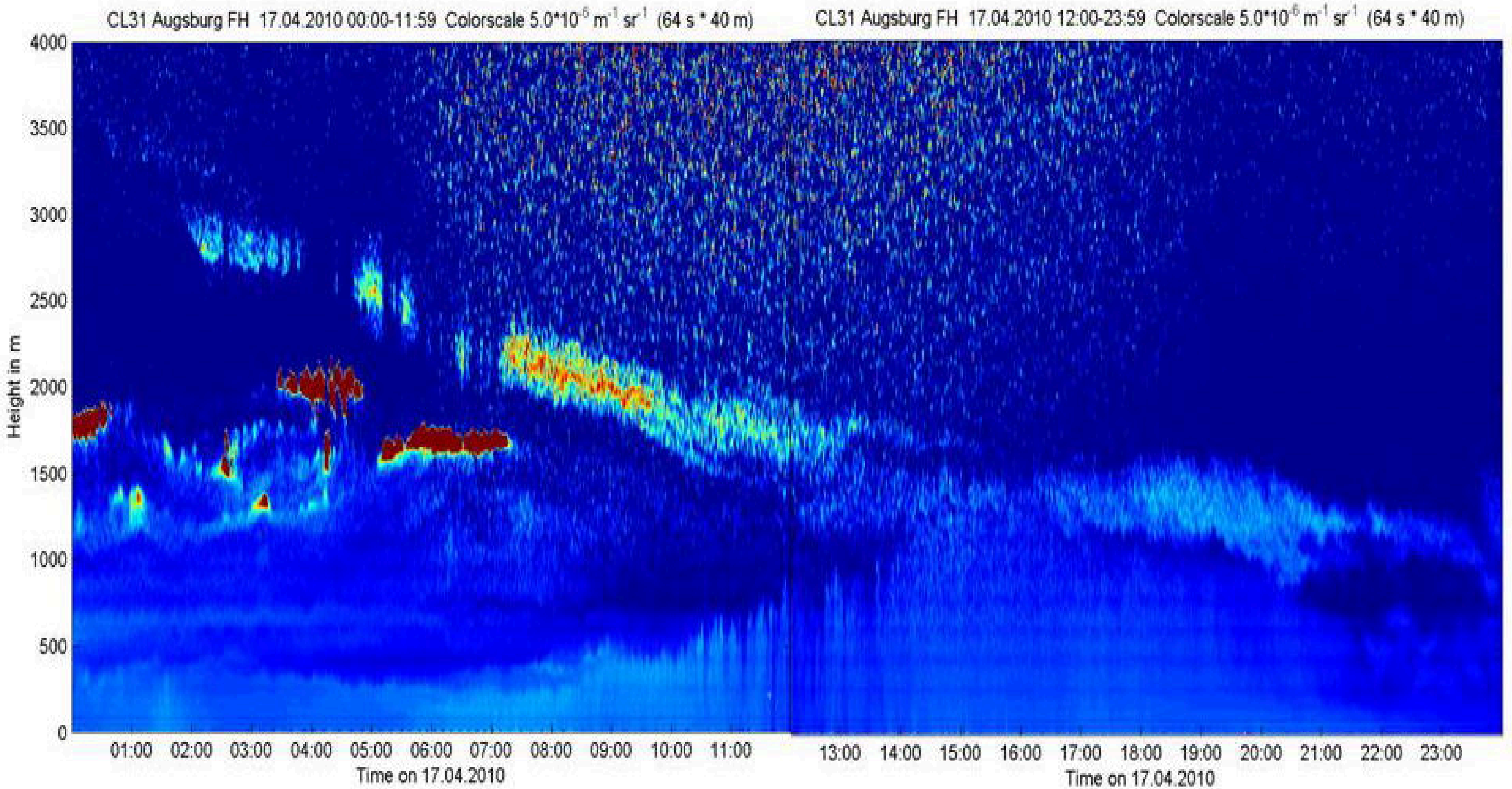

read more: Emeis, S., R. Forkel, W. Junkermann, K. Schäfer, H. Flentje, S. Gilge, W. Fricke, M. Wiegner, V. Freudenthaler, S. Groß, L. Ries, F. Meinhardt, W. Birmili, C. Münkel, F. Obleitner, P. Suppan, 2011: Measurement and simulation of the 16/17 April 2010 Eyjafjallajökull volcanic ash layer dispersion in the northern Alpine region. Atmos. Chem. Phys., 11, 2689–2701

RASS

principles of operation

examples

RASS, acoustic, electro-magnetic backscatter, ➔ wind and temperature profiles

RASS: frequencies

Bragg condition:
acoustic wavelength = ½ electro-magnetic wavelength

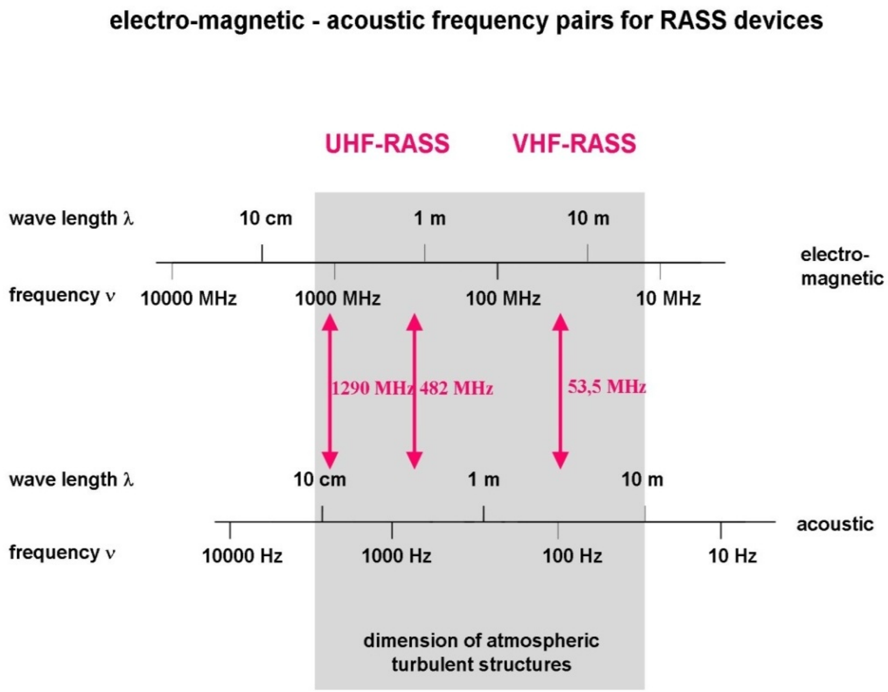

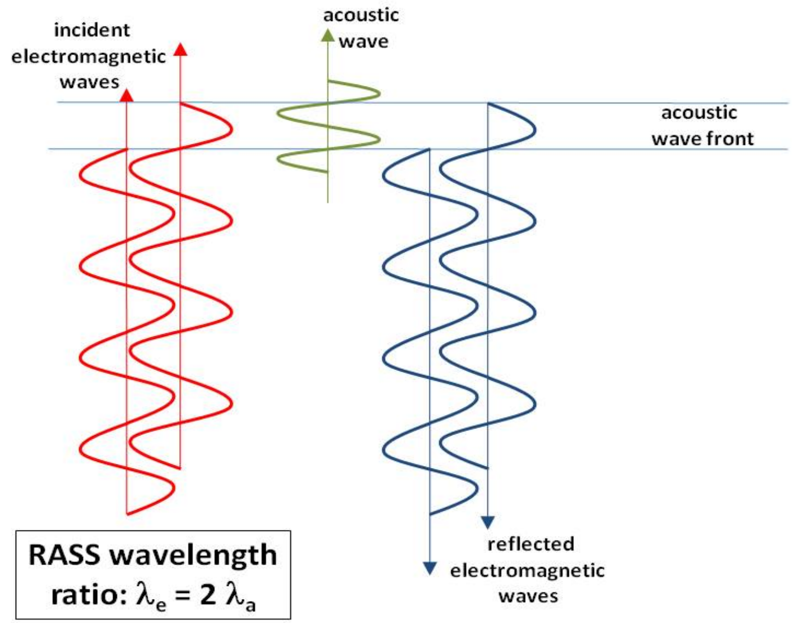

Emeis, S., 2010: Measurement Methods in Atmospheric Sciences - In situ and remote. Borntraeger, Stuttgart, 272 pp., 103 figs, 28 tables, ISBN 978-3-443-01066-9.

RASS measuring principle

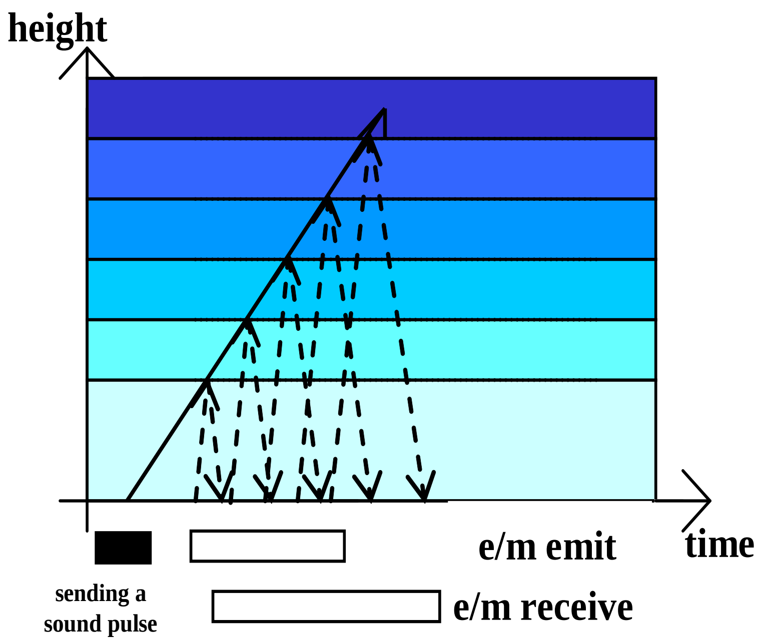

detection:

travel time of em./ac. signal	= height	
ac. backscatter intensity	= turbulence	(identical to SODAR)
ac. Doppler-shift	= line-of-sight wind speed	(identical to SODAR)
em. Doppler shift	= sound speed ➔ temperature	

RASS (radio-acoustic remote sensing)

measures vertical temperature profiles

Bragg-RASS: windprofiler plus acoustic component

Doppler-RASS: SODAR plus electro-magnetic component

UHF RASS (boundary layer)

VHF RASS (troposphere)

SODAR-RASS (Doppler-RASS) (METEK)

acoustic frequ.: 1077 Hz
radio frequ.: 474 MHz
resolution: 20 m
lowest
range gate: ca. 40 m

vertical range: 540 m

Bragg-RASS

acoustic frequ.: about 3000 Hz
radio frequ.: 1290 MHz
resolution: 50 m
lowest
range gate: ca. 200 m

vertical range: 1000 m

sample RASS data: summer day
potential temperature (left), horizontal wind (right)

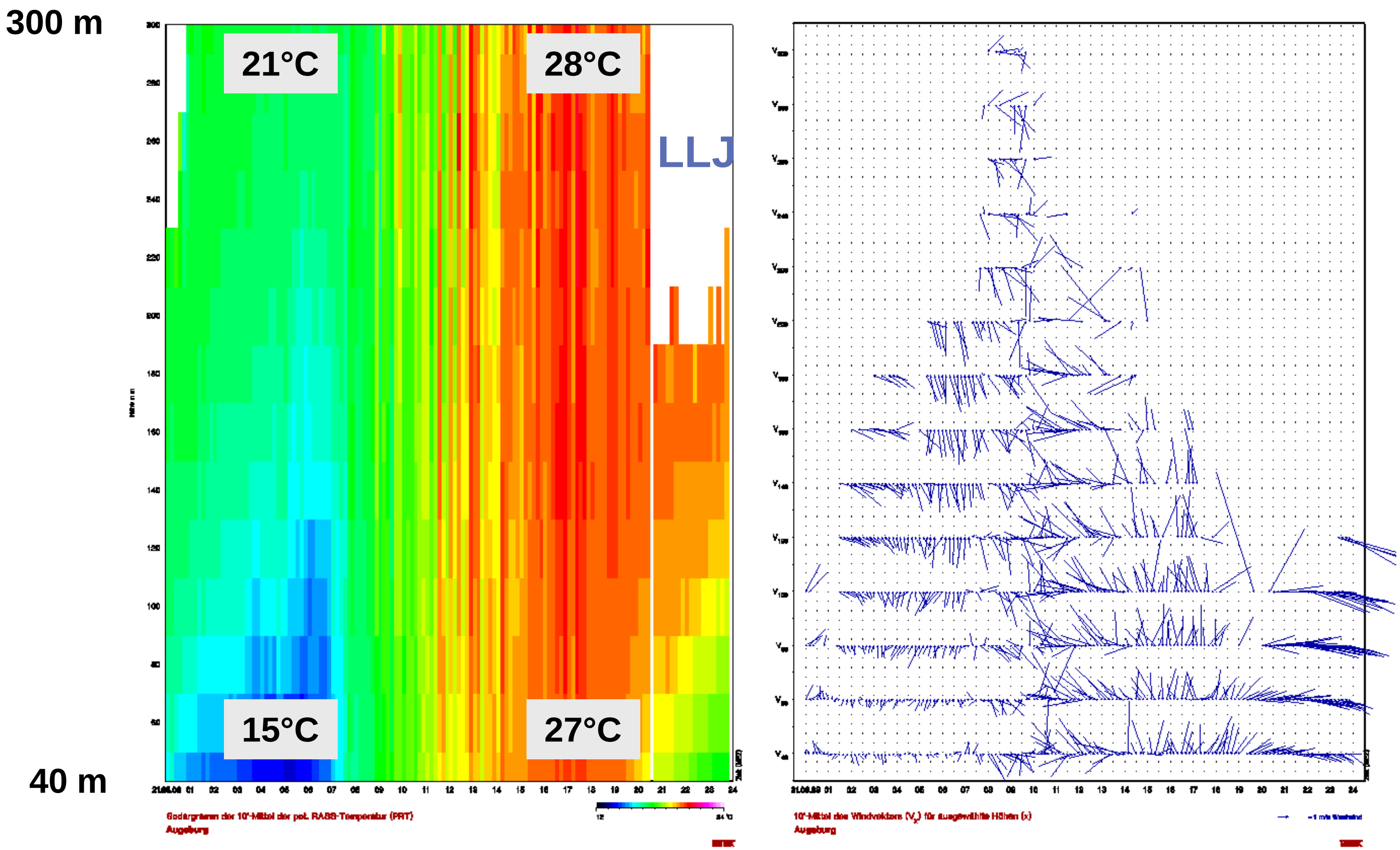

Institute for Meteorology and Climate Research –
Atmospheric Environmental Research

sample RASS data: winter day
potential temperature (left), horizontal wind (right)

300 m

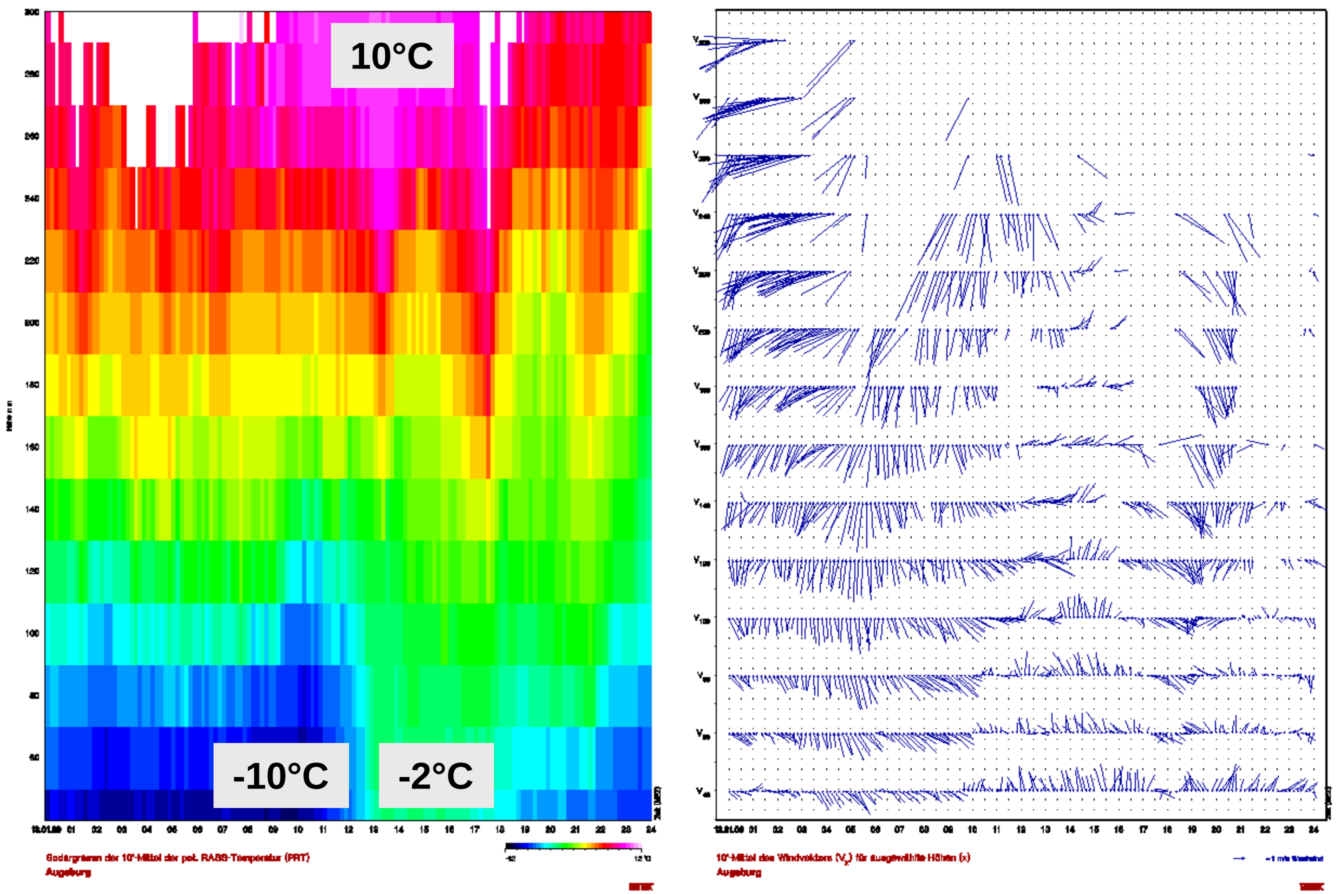

40 m

Doppler windlidar

wind, turbulence, aerosol detection, mixing-layer height, low-level jet

Wind-LIDAR, optical backscatter, Doppler shift analysis, wave length ~ 1.5 µm
➔ wind and aerosol profiles

range detection by
moving focus

range detection by
run time

Doppler windlidar measuring principle

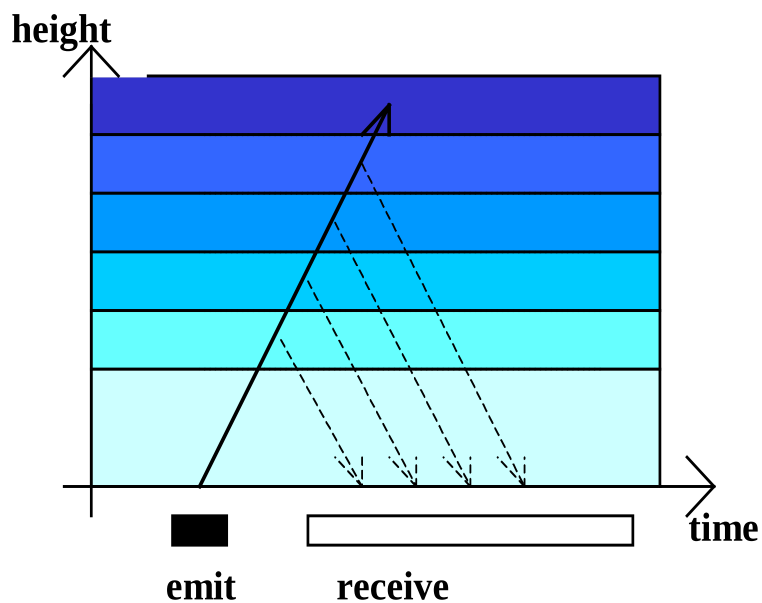

detection:

travel time of signal = height
backscatter intensity = particle size and number distribution
depolarisation = particle shape
Doppler-shift = wind speed in the line of sight

Doppler-beam-swinging (DBS) technique

(SODAR)

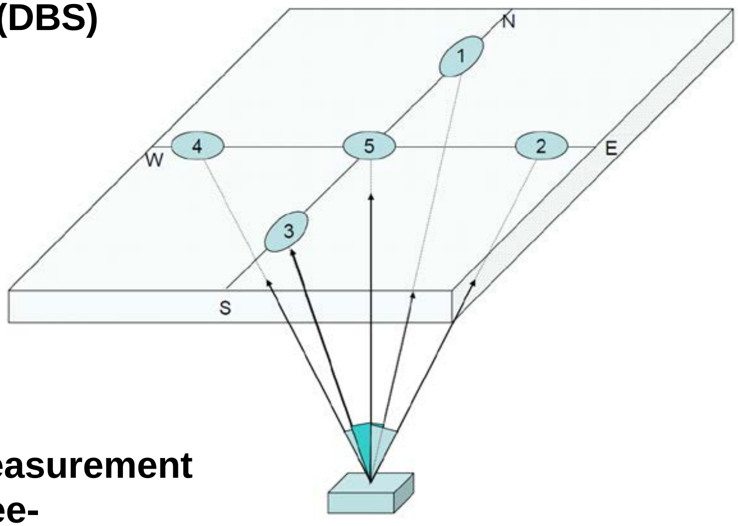

for the measurement of the three-dimensional wind vector

conical scanning technique

(Lidar)

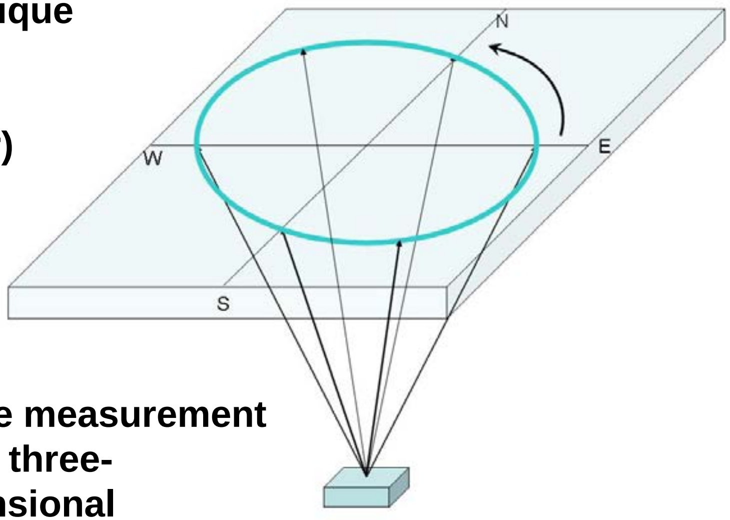

for the measurement of the three-dimensional wind vector

range detection by moving focus

focal range gets longer at larger ranges

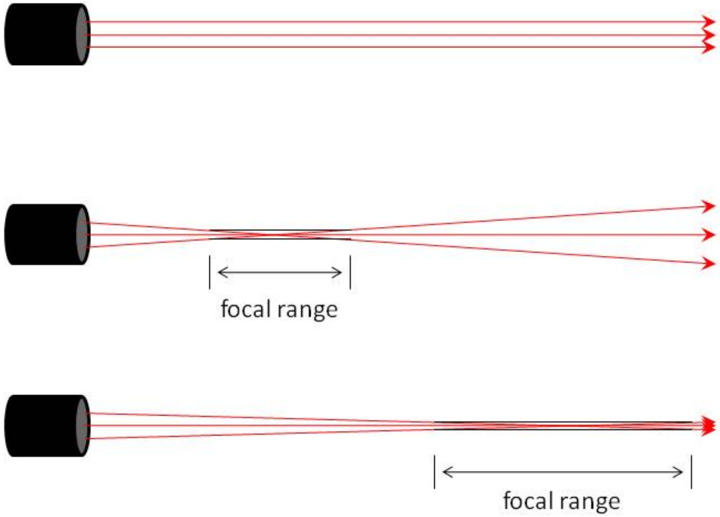

Sample measurement: Yatir Forest, Israel

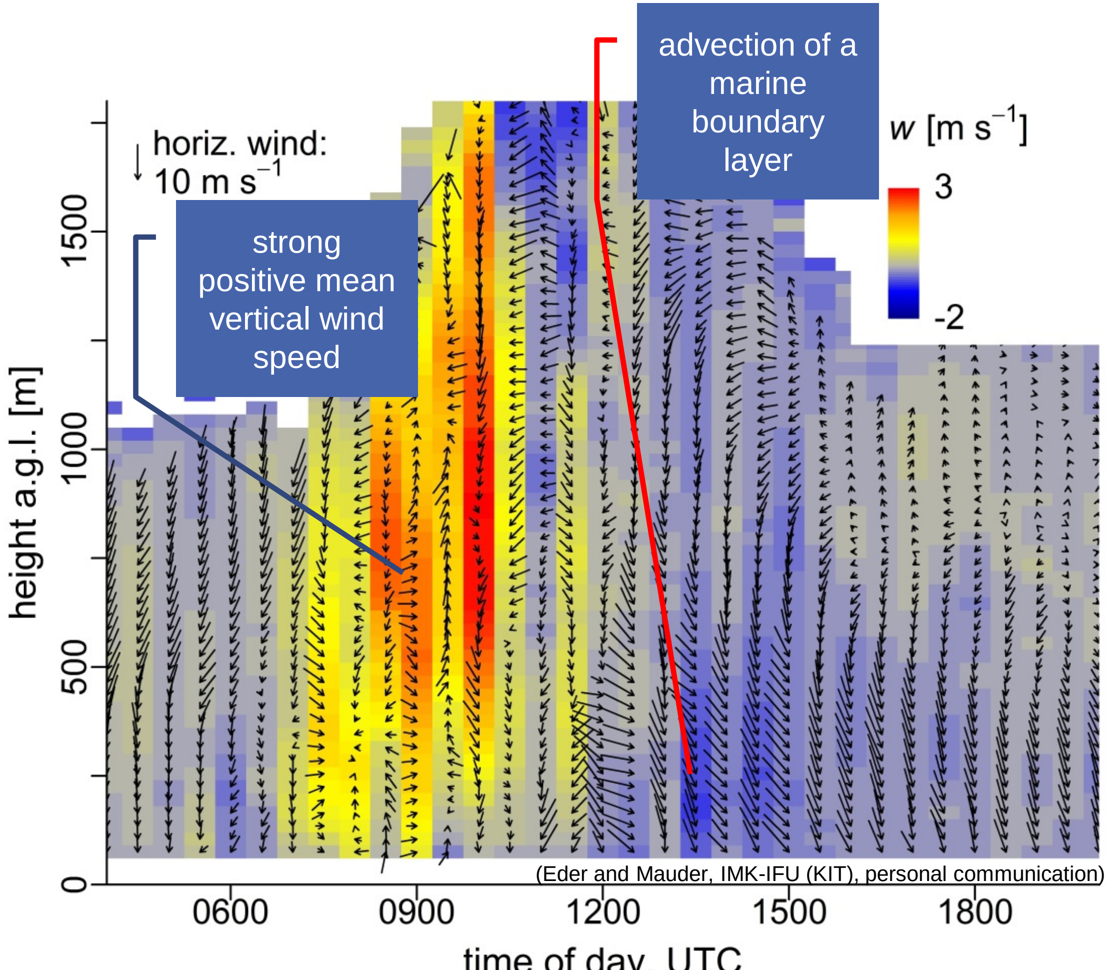

The 3-d wind field above the Yatir forest on 10 Sept 2013. The colour indicates the vertical wind component. The black arrows indicate the horizontal wind component: the direction of the arrow shows the wind direction, the length of the arrow shows the wind speed.

During the afternoon hours, there is a 180°-shift in wind direction between surface and boundary-layer top which indicates a stationary circulation. Please note that this picture is not shown in local time, but in UTC (i.e. 12:00 means 14:00 Israel winter time)

conical scanning assumes horizontal homogeneity, but:

Karlsruhe Institute of Technology

THE UNIVERSITY OF AUCKLAND
NEW ZEALAND

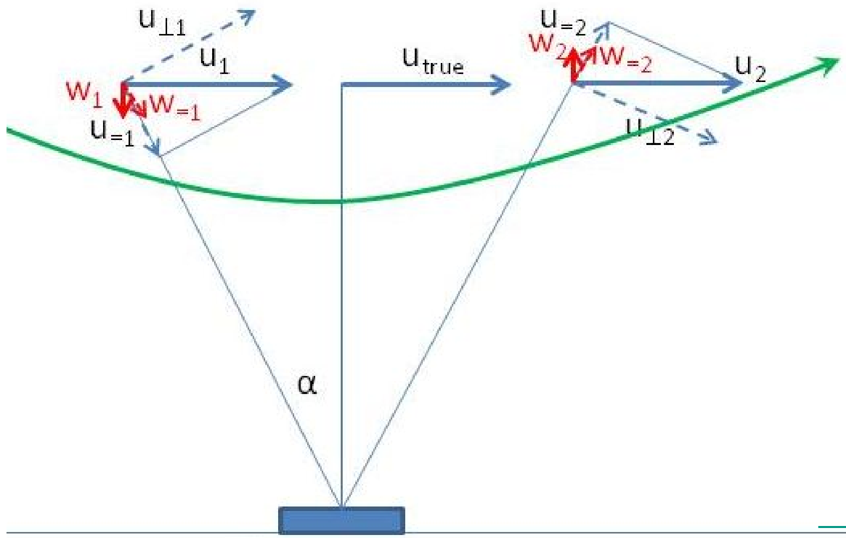

valley:

w-component adds to u-component

➔ SODAR/LIDAR measures too much wind

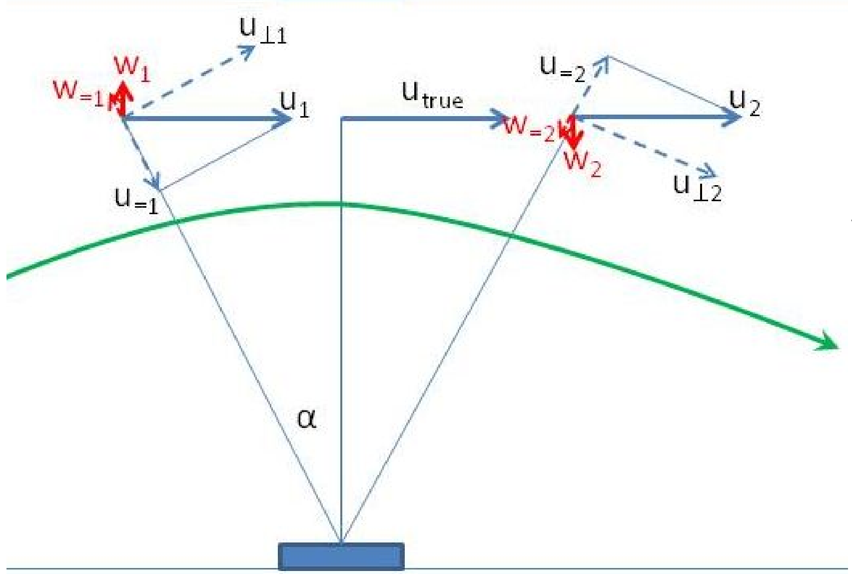

hill top / pass:

w-component reduces u-component

➔ SODAR/LIDAR measures too little wind

interesting for complex terrain

three wind lidars ➔ virtual tower

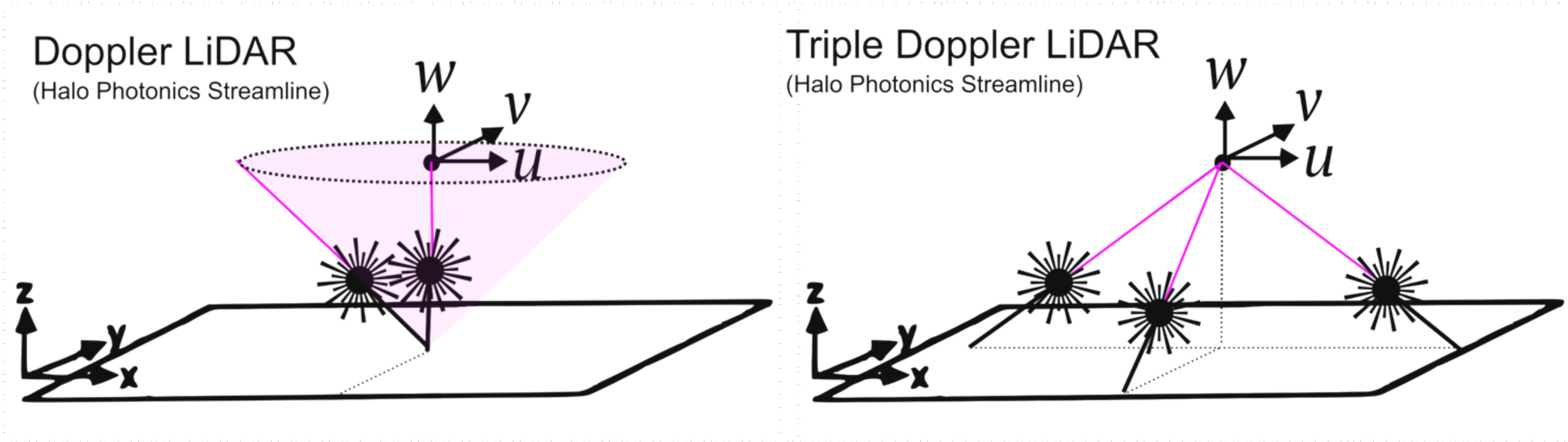

☺☺☺💣 **RASS delivers temperature profiles, wind profiles are additionally available.**
MLH directly from temperature profiles. LLJ from wind profiles.
<u>Does not work properly</u> under high wind speeds. Restricted range.

☺☺☺💣 **wind lidar detects wind profiles, aerosol distribution and water droplets. It has to be assumed that the aerosol follows the thermal structure of the atmosphere and the wind.**
MLH from aerosol backscatter, wind speed variance, LLJ from wind profiles.
<u>Does not work properly</u> in extreme clear (aerosol-free) air and during precipitation events and fog.

☺☺💣💣 **Ceilometer detects aerosol distribution and water droplets. It has to be assumed that the aerosol follows the thermal structure of the atmosphere.**
MLH indirectly from aerosol backscatter using a MLH algorithm.
<u>Does not work properly</u> in extreme clear (aerosol-free) air and during precipitation events and fog.

☺💣💣💣 **SODAR detects wind profiles, temperature fluctuations and gradients, but no absolute temperature.**
MLH indirectly from acoustic backscatter (MLH algorithm). LLJ from wind profiles.
<u>Does not work properly</u> under perfectly neutral stratification, with very high wind speeds, and during stronger precipitation events. Restricted range.

Options for offshore wind farms

buoys, oil rigs, satellites, …

Offshore measurements

In situ: masts

remote sensing: wind lidar on platforms

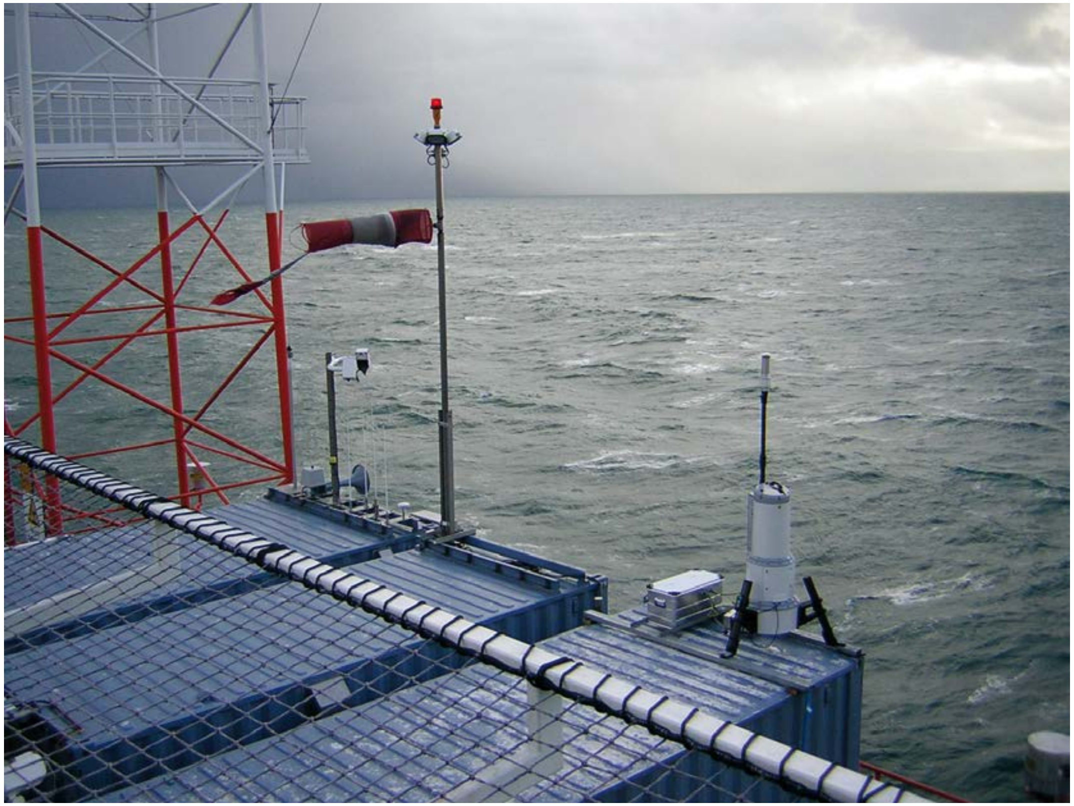

http://www.zephirlidar.com/zephir-lidar-products/gallery/

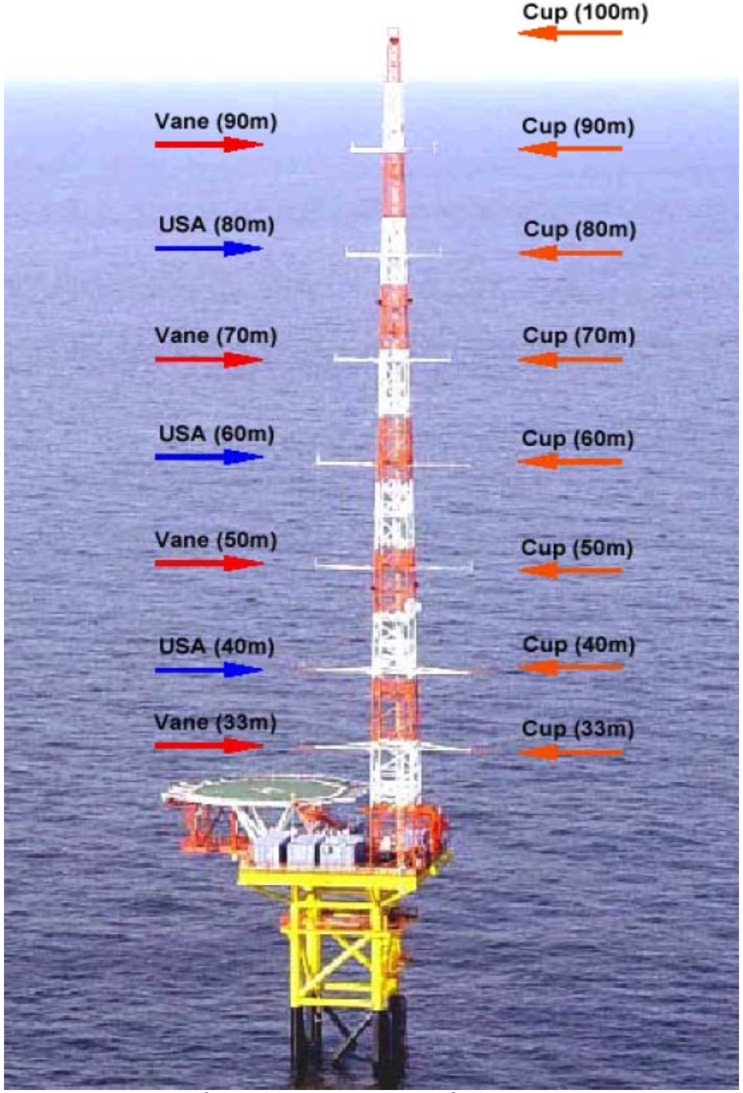

Neumann, T., K. Nolopp, 2007: DEWI-Magazin 30,
http://www.dewi.de/dewi_res/fileadmin/pdf/publications/Magazin_30/08.pdf

Offshore measurements

remote sensing: high-resolution wind lidar on ships

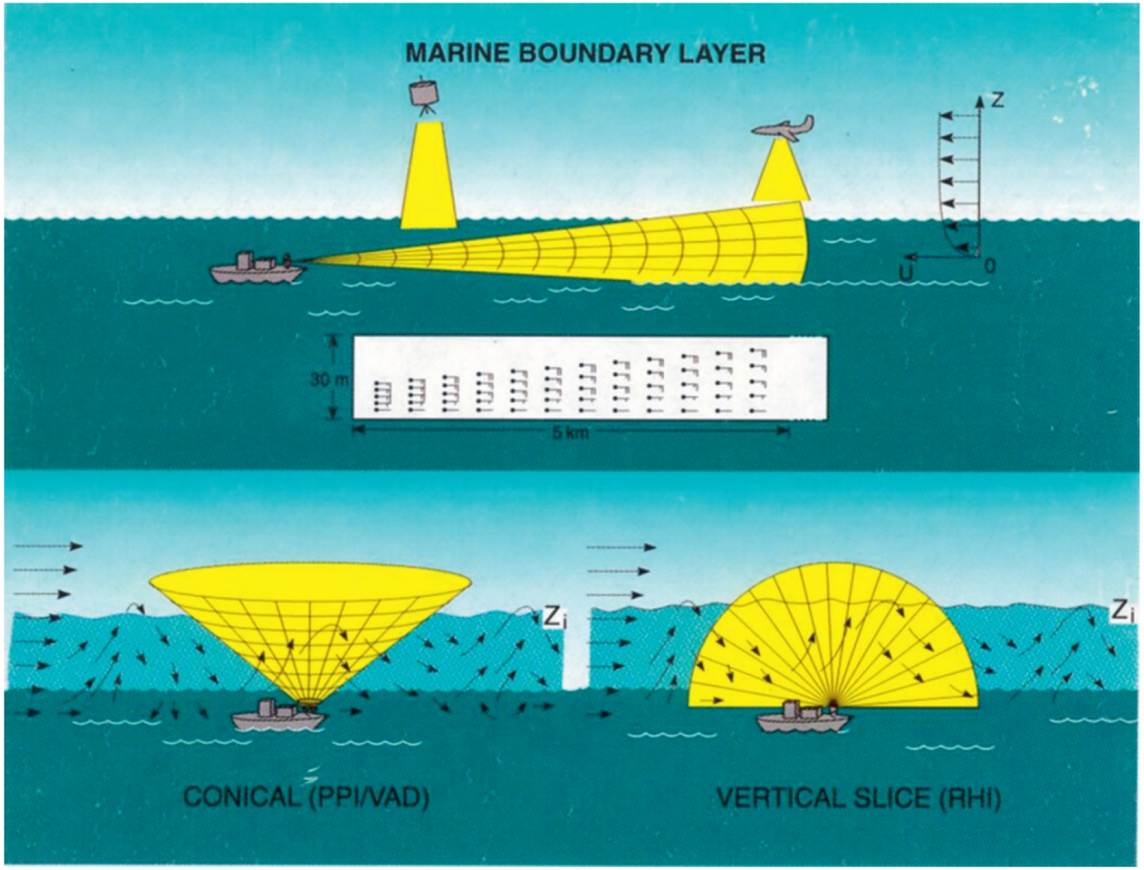

FIG. 2. Common scanning patterns used by HRDL: (top) elevation sector or "vertical slice" scan, (bottom left) azimuth or conical scan at a fixed elevation angle, and (bottom right) full 180° elevation vertical-slice scan.

Pichugina, Y. L., Banta, R. M., Brewer, W. A., Sandberg, S. P., & Hardesty, R. M., 2012: Doppler lidar-based wind-profile measurement system for offshore wind-energy and other marine boundary layer applications. *Journal of Applied Meteorology and Climatology*, *51*, 327-349.

Offshore measurements

remote sensing: wind lidar on buoys (Flidar)

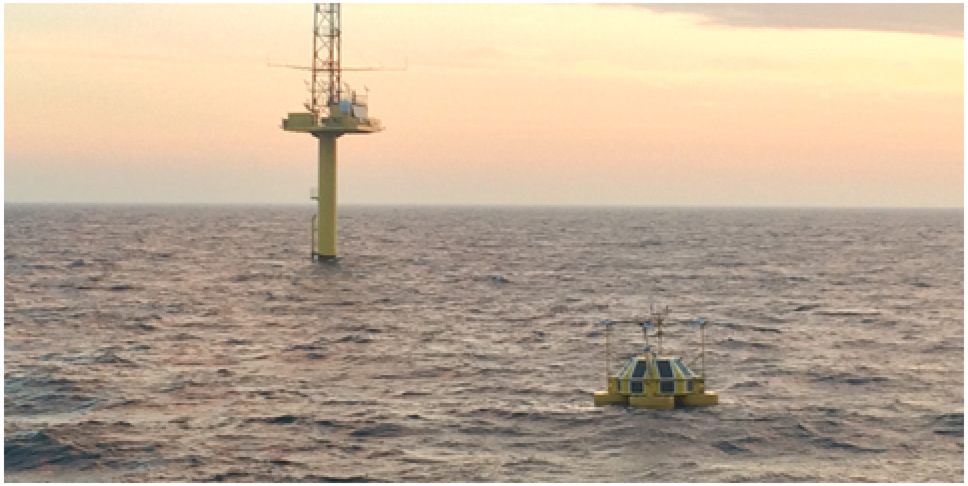

http://www.rwe.com/web/cms/de/86182/rwe-innogy/presse-news/pressemitteilung/?pmid=4014556

Flidar: **http://www.offshorewind.biz/2014/11/19/flidar-joins-norcowe/**

Satellite-based remote sensing

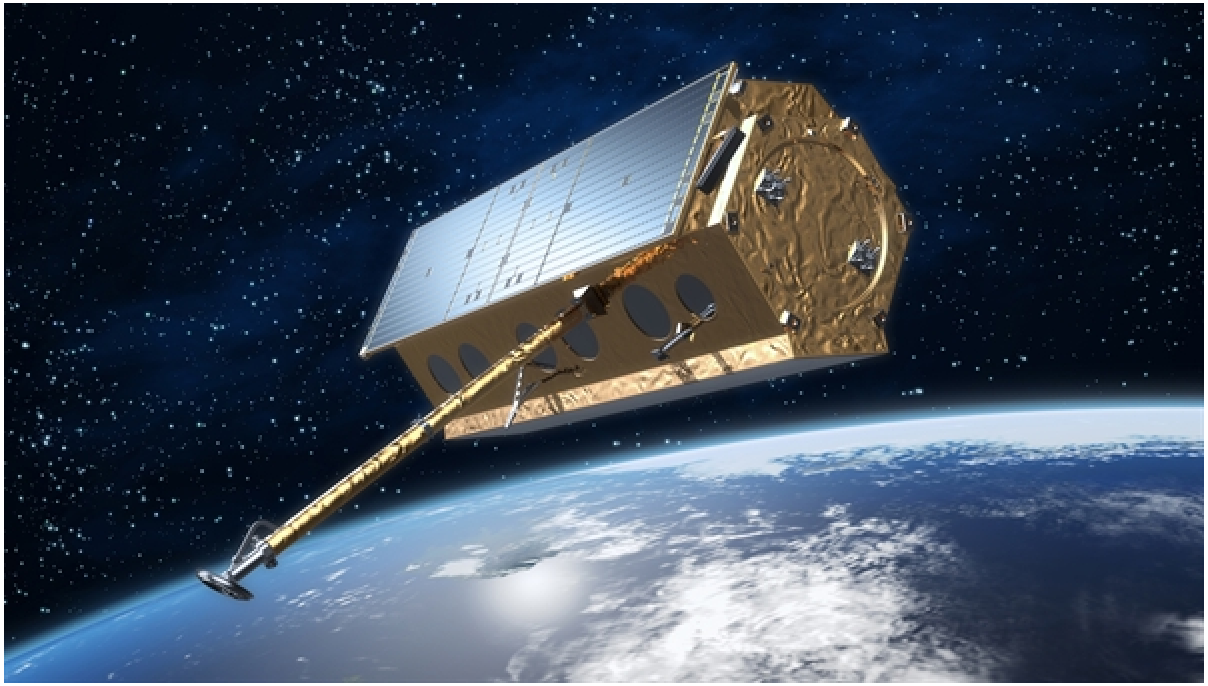

http://www.dlr.de/dlr/desktopdefault.aspx/tabid-10377/565_read-436/#/gallery/350

observations day and night, also through clouds

TerraSAR-X at a glance:

Size:	4.88 metre
Diameter:	2.4 metre
Weight:	1 230 kilogramme
Payload:	ca. 400 kilogramme
Radar frequency:	9.65 GigaHertz
Power:	800 Watt (averaged)
Resolution:	1 metre, 3 metre, 16 metre (abhängig von der Bildgröße)
Carrier rocket:	Dnepr 1 (former SS-18)
Start:	15 Juni 2007, 4:14 GMT+2
Launch site:	Baikonur, Kasachstan
Height:	514 kilometres
Inclination angle against the Equator:	97.4 degrees (sun synchronised)
Life expectancy:	at least 5 years

Satellite-based remote sensing

https://sentinel.esa.int/web/sentinel/missions/sentinel-1/overview

Sentinel-1 at a glance:

Weight:	2 300 kilogramme
Radar frequency:	5.405 GigaHertz
Power:	5 900 Watt (averaged)
Resolution:	5x5 metre, 5x20 metre, 5x40 metre (depending on image size)
Start:	April 2014
Orbit:	
Height:	693 kilometres
Inclination angle against the Equator:	98.18 degrees (sun synchronised)
Life expectancy:	at least 12 years

Satellite-based remote Sensing

Sentinel-1 revisit frequency (two satellites)

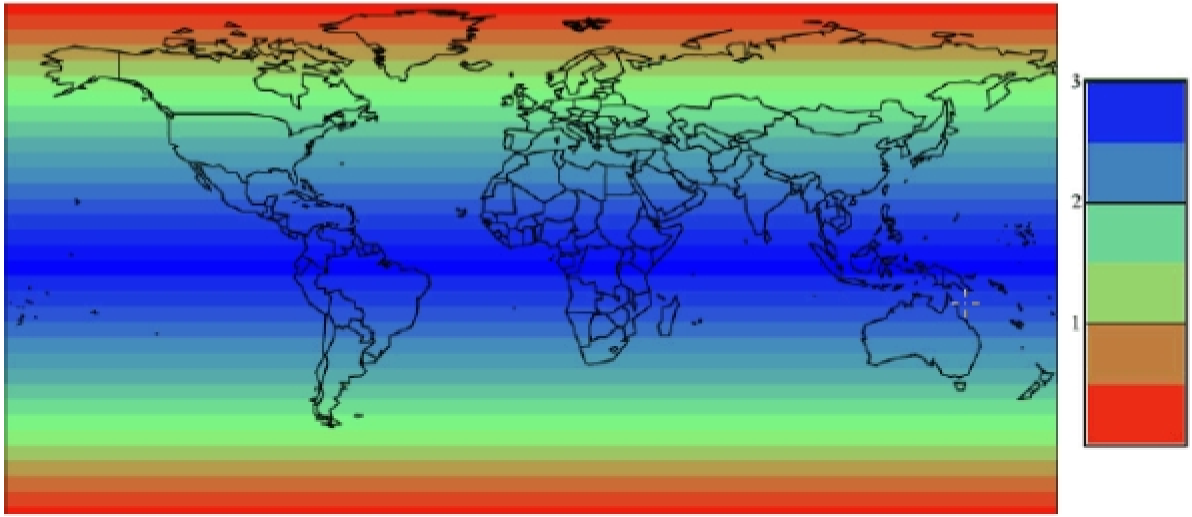

- ✓ Two satellites in a 12 day orbit
- ✓ Repeat frequency: 6 days (important for coherence)
- ✓ Revisit frequency: (asc/desc & overlap): 3 days at the equator, <1 day at high latitudes (Europe ~ 2 days)

https://sentinel.esa.int/web/sentinel/user-guides/sentinel-1-sar/revisit-and-coverage

Satellite-based remote sensing

Synthetic Aperture

extensive computer processing of subsequent data allows for an artificial aperture of up to 15 km

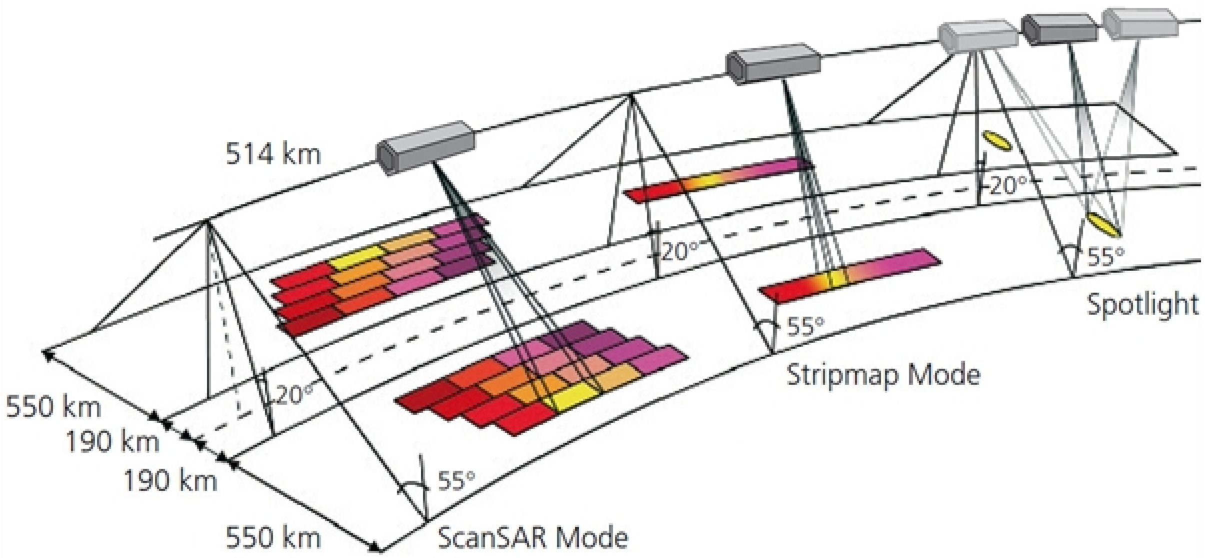

http://www.dlr.de/dlr/de/desktopdefault.aspx/tabid-10382/570_read-431/#/gallery/356

Satellite-based remote sensing

SAR images – basic principle of speed measurement

smooth sea surface
no return

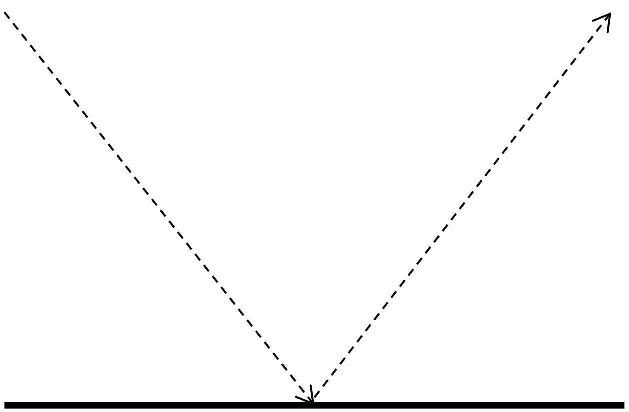

capillary waves on sea surface
best return on Bragg condition

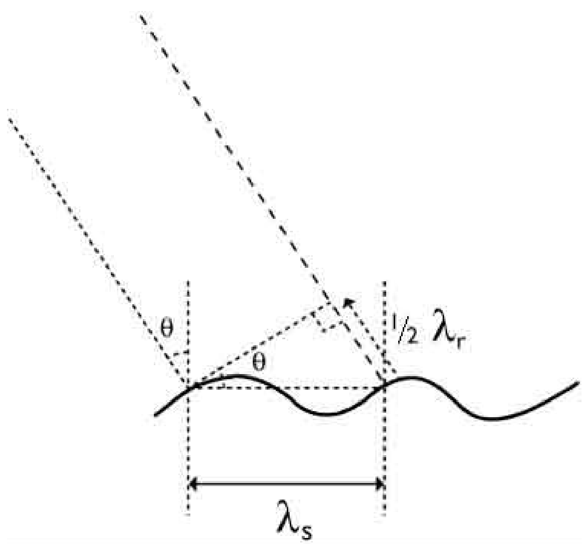

https://earth.esa.int/web/guest/missions/esa-operational-eo-missions/ers/instruments/sar/applications/radar-courses/content-2/-/asset_publisher/qIBc6NYRXfnG/content/radar-course-2-bragg-scattering

Satellite-based remote sensing

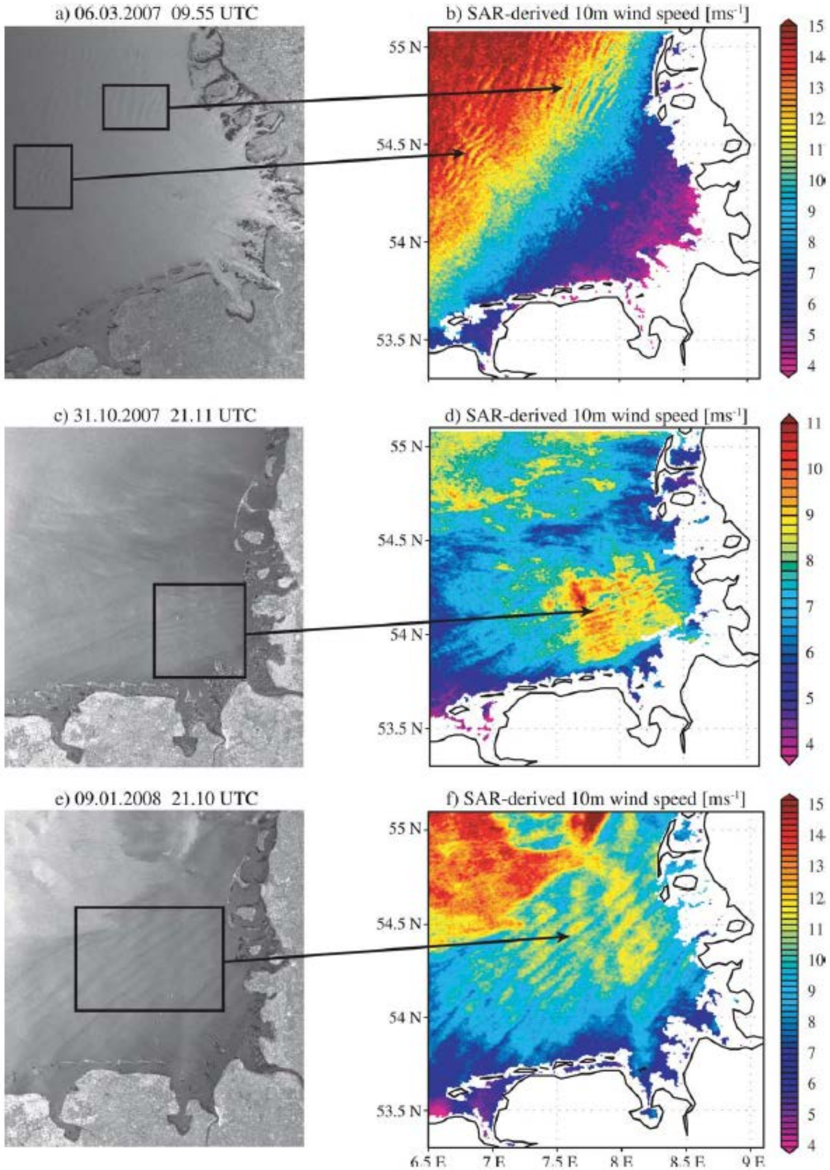

wind speed fields at 10 m height in the German Bight from SAR data for three different weather situations

Source: Müller, S. E.V. Stanev, J. Schulz-Stellenfleth, J. Staneva, W. Koch, 2013: Atmospheric boundary layer rolls: Quantification of their effect on the hydrodynamics in the German Bight. JGR 118, 5036–5053.

Satellite-based remote sensing

Inversion procedure

SAR data ➔ Normalised radar cross-section (NRCS)

➔ Geophysical Model Function (GMF)

➔ u_{10} as function of wind direction, antenna view angle, incident angle

Li and Lehner 2014: Algorithm for Sea Surface Wind Retrieval From TerraSAR-X and TanDEM-X Data. IEEE TRANSACTIONS ON GEOSCIENCE AND REMOTE SENSING, VOL. 52, NO. 5, MAY 2014, 2928-2939.

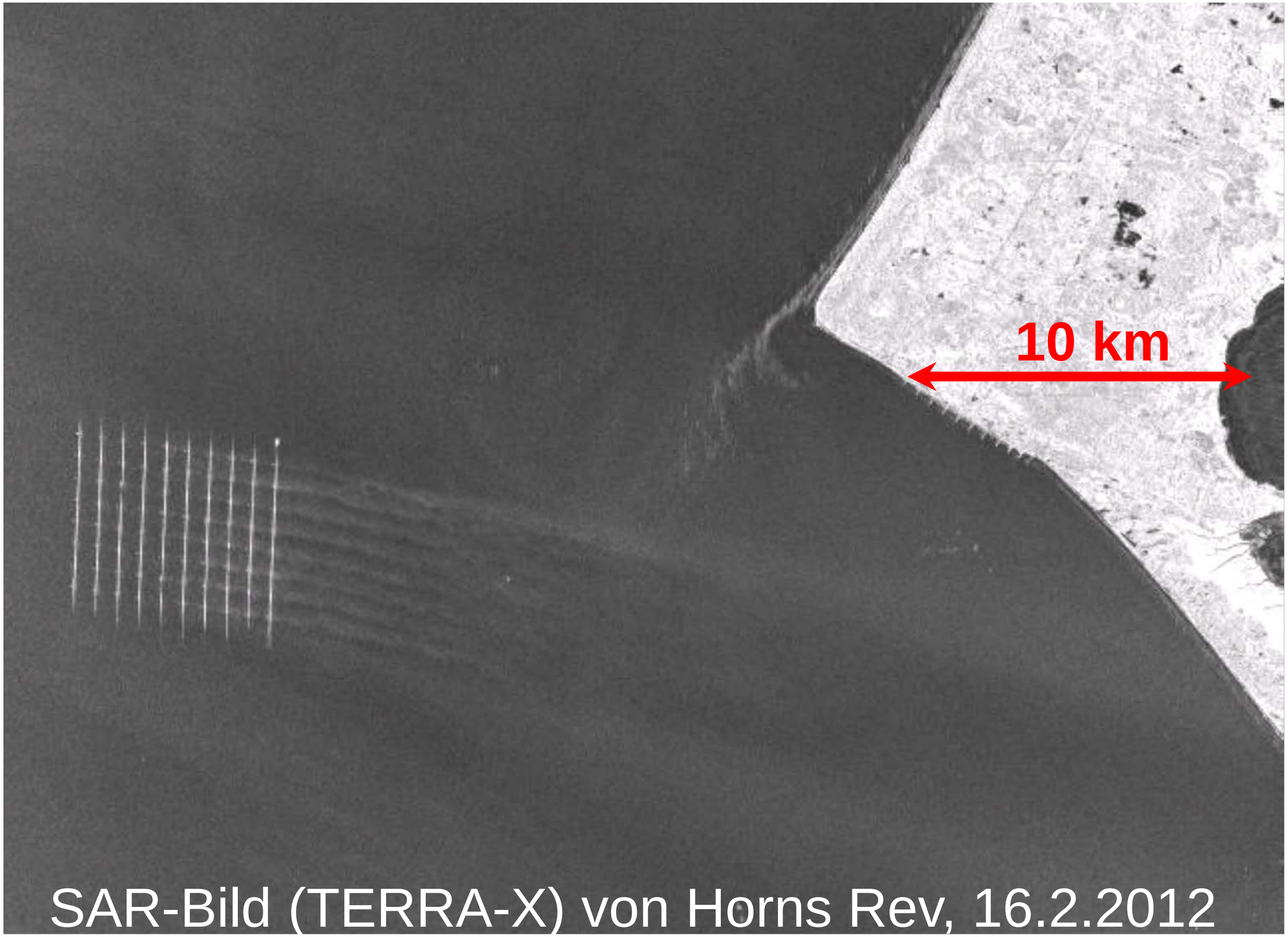

(c) DLR 2012
TerraSar-X

Alpha Ventus 12. August 2012, 05:51 UTC

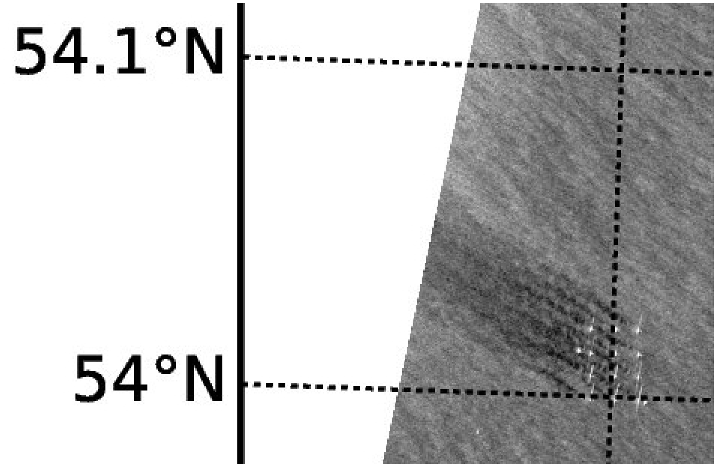

(c) TerraSAR-X, DLR 2012

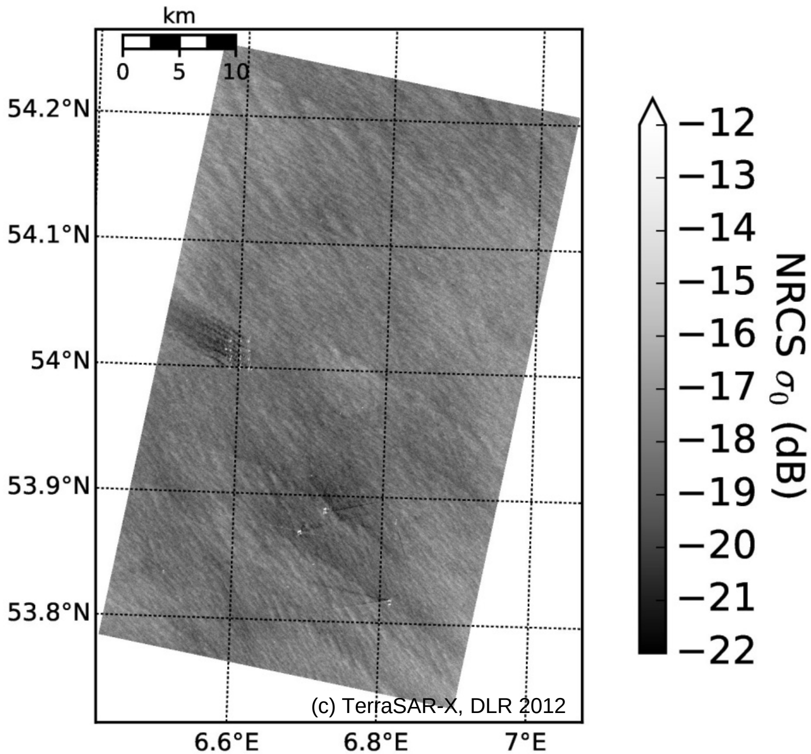

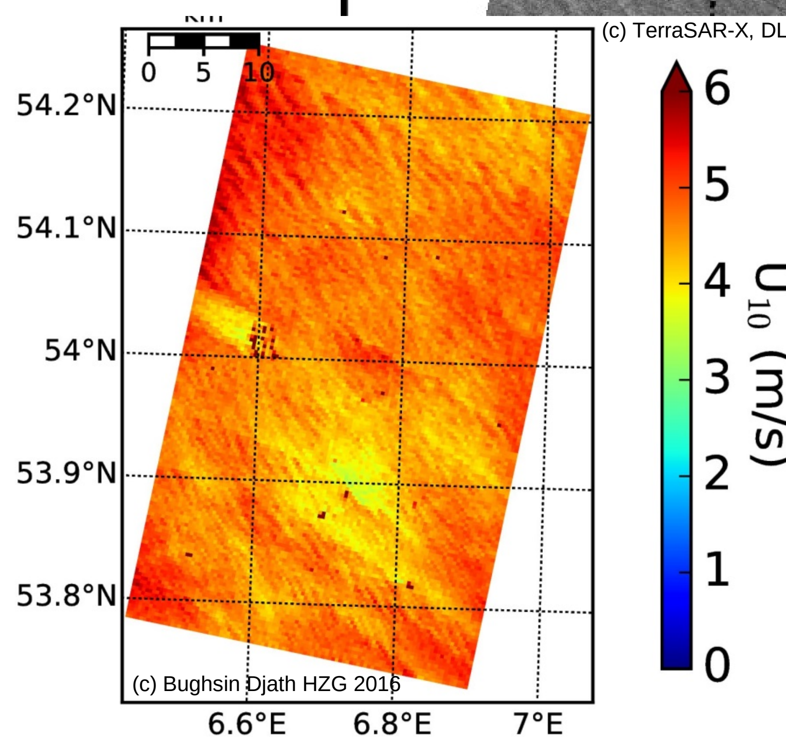

North Sea
3 Juni 2015, 17:16 UTC

http://www.ofw-online.de/projekte/nordseekarte.html

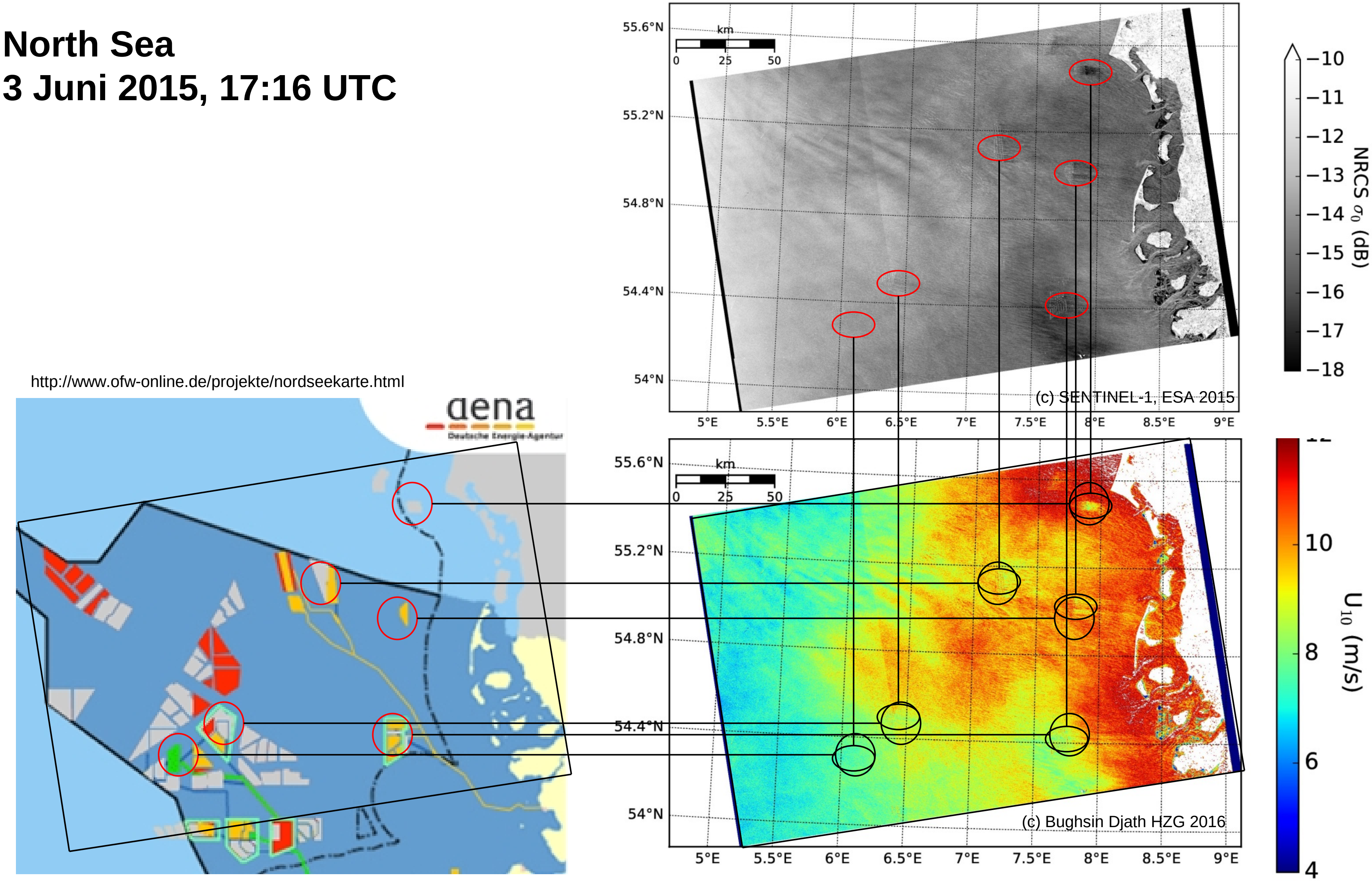

Offshore: Wind profile depending on SST – air temperature difference

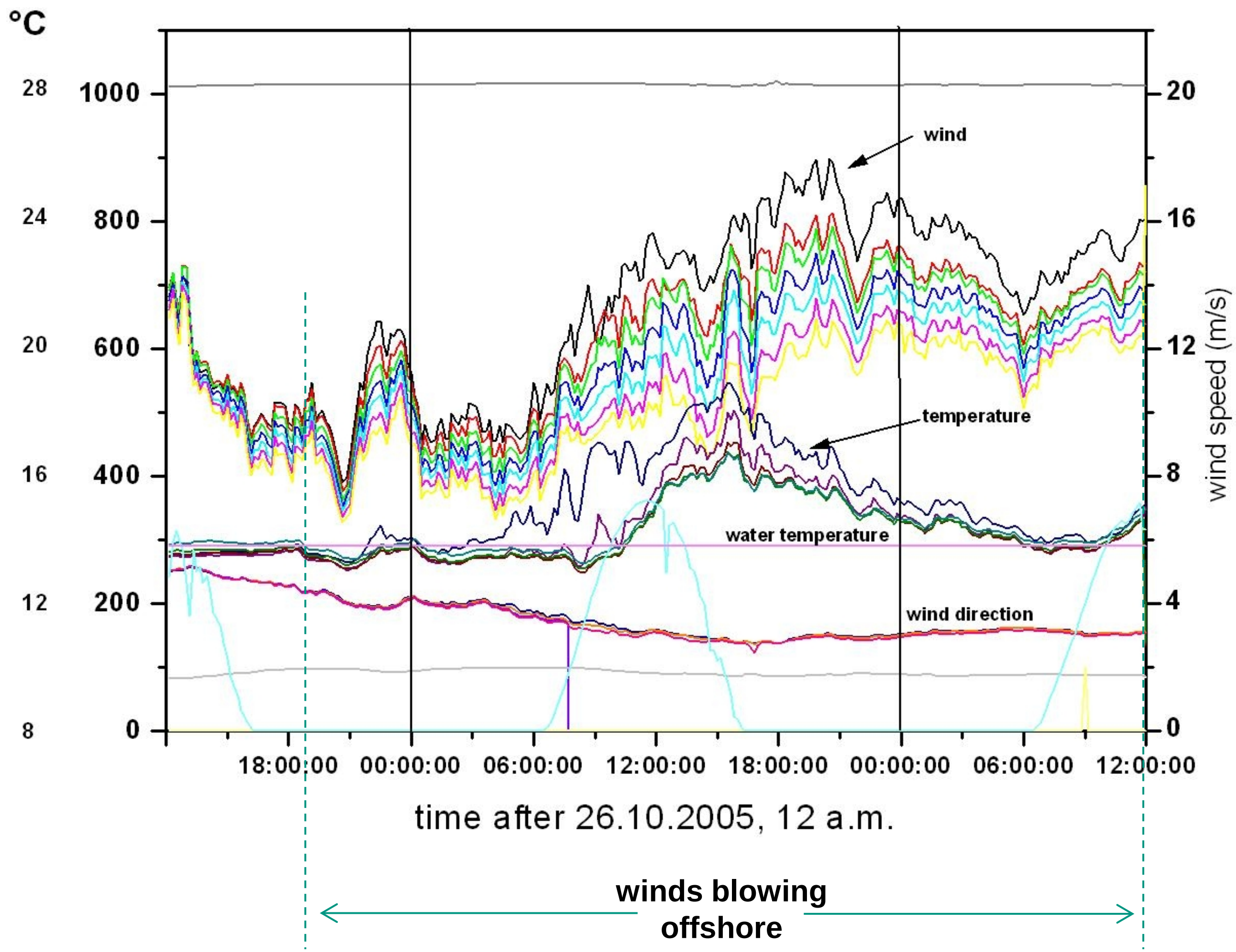

offshore: humidity profile contributes to unstable stratification (FINO1 41.5 m data for turb. heat and humidity fluxes)

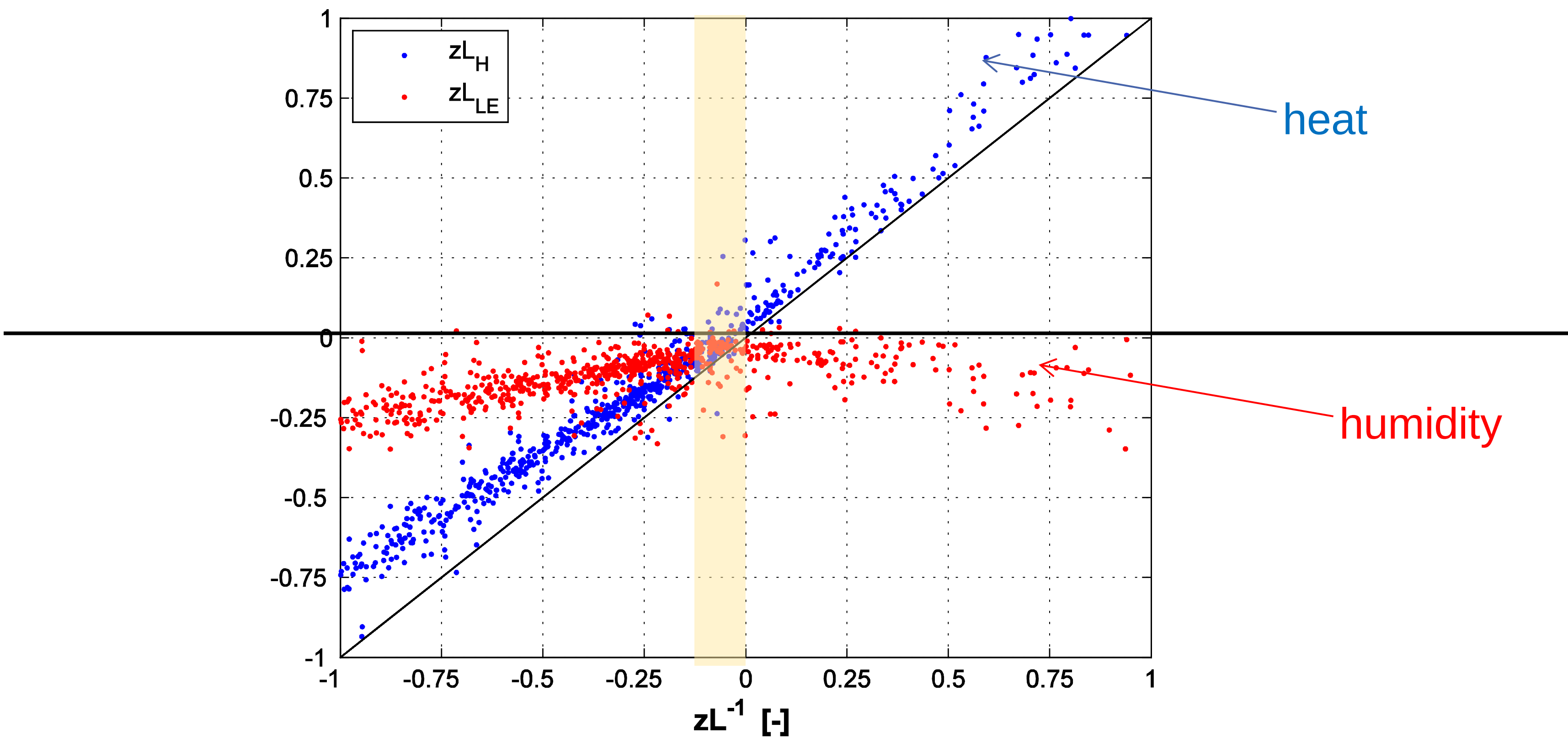

Source: RAVE-Project TUFFO, Richard Foreman

Aircraft measurements Four flight campaigns, two in spring and two in autumn are scheduled in order to assess the extension and characteristics of wind farm wake far fields.

The DO 128 of the Technical University of Braunschweig

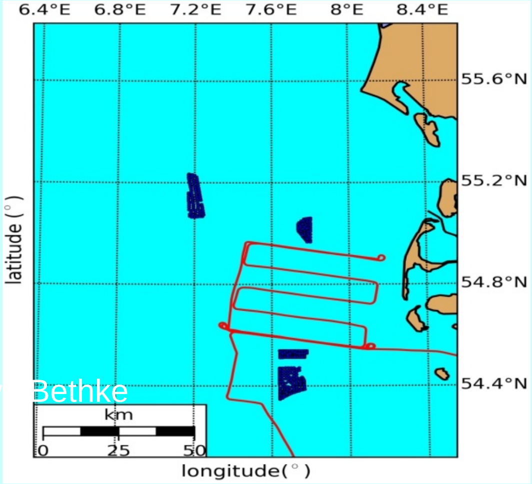

Far wake flight pattern

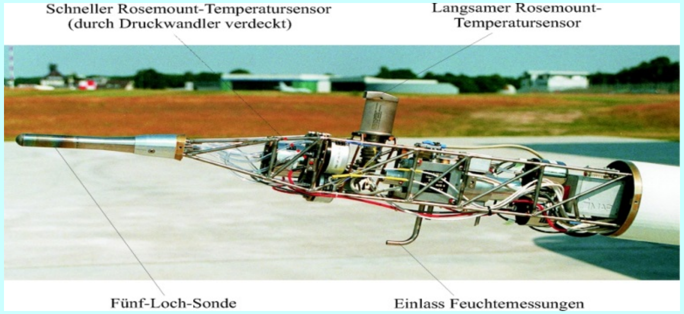

Instrumentation of the nose boom:
- temperature
- humidity
- turbulence (5 hole probe)

Gefördert durch:
Bundesministerium für Wirtschaft und Energie
aufgrund eines Beschlusses des Deutschen Bundestages

Newly started research project WIPAFF
(WInd PArk Far Fields)

11.2015 – 02.2019

5 Partners:	**KIT, Institute of Meteorology and Climate Research**
	Technical University of Braunschweig
	Helmholtz Centre Geesthacht
	UL International GmbH (ex: DEWI)
	University of Tübingen

Aircraft (Do 128) observations in the wakes
Analysis of satellite SAR data of wakes
Mesoscale wind field modelling with WRF (wave model, park parametrisation)
Adjustment of analytic and industrial wind park models

assessment of impact on regional climate

Impact on regional climate

cloud formation,
modification of precipitation patterns
modification of sun shine duration
modification of wind fields
…

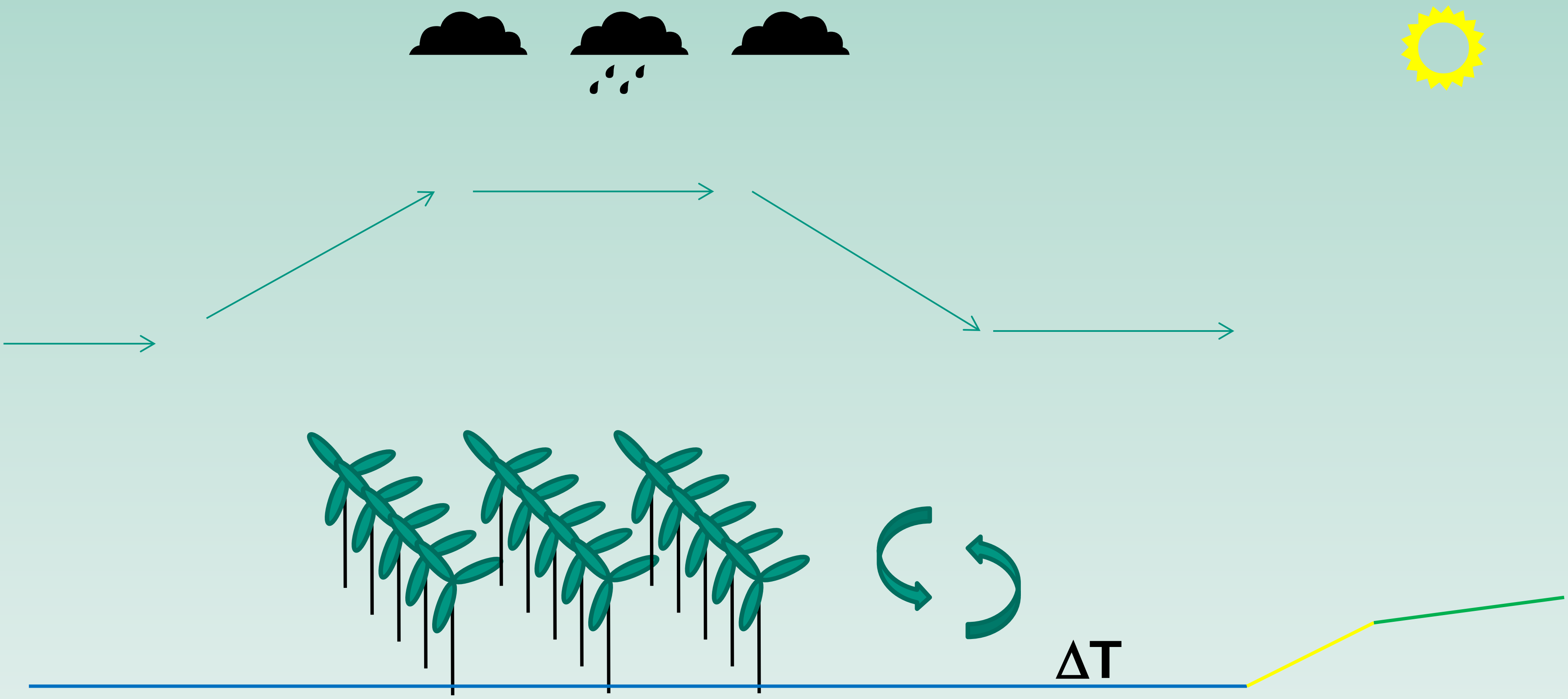

airborne measurement system at IMK-IFU: drone (hexacopter)

➔ see afternoon lecture

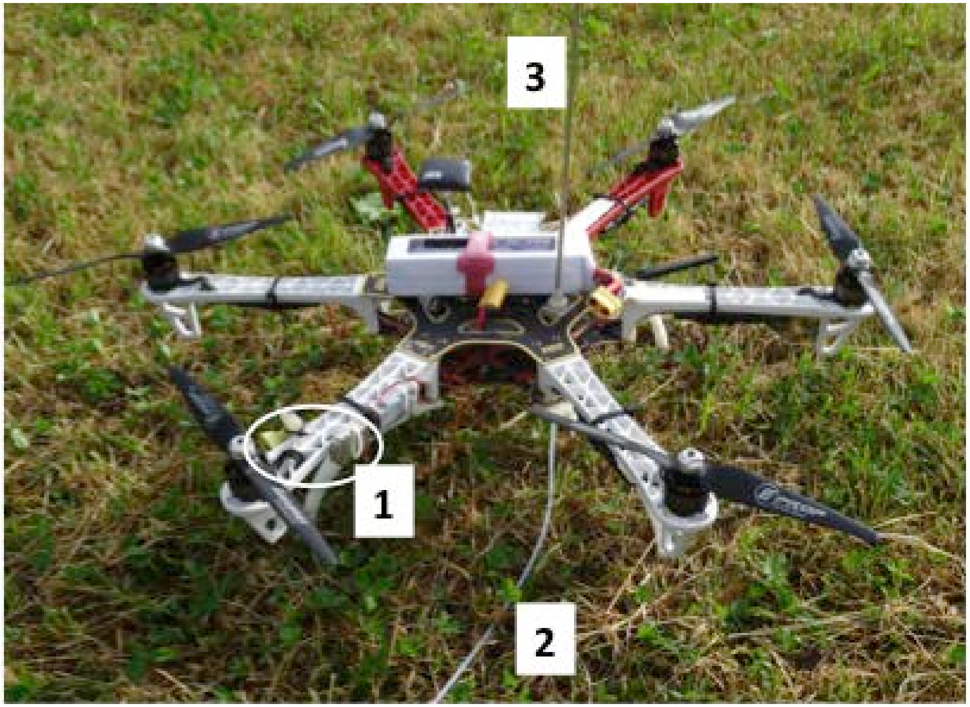

1 Air temperature and humidity sensors

2 Teflon tube

3 Tube extension above hexacopter

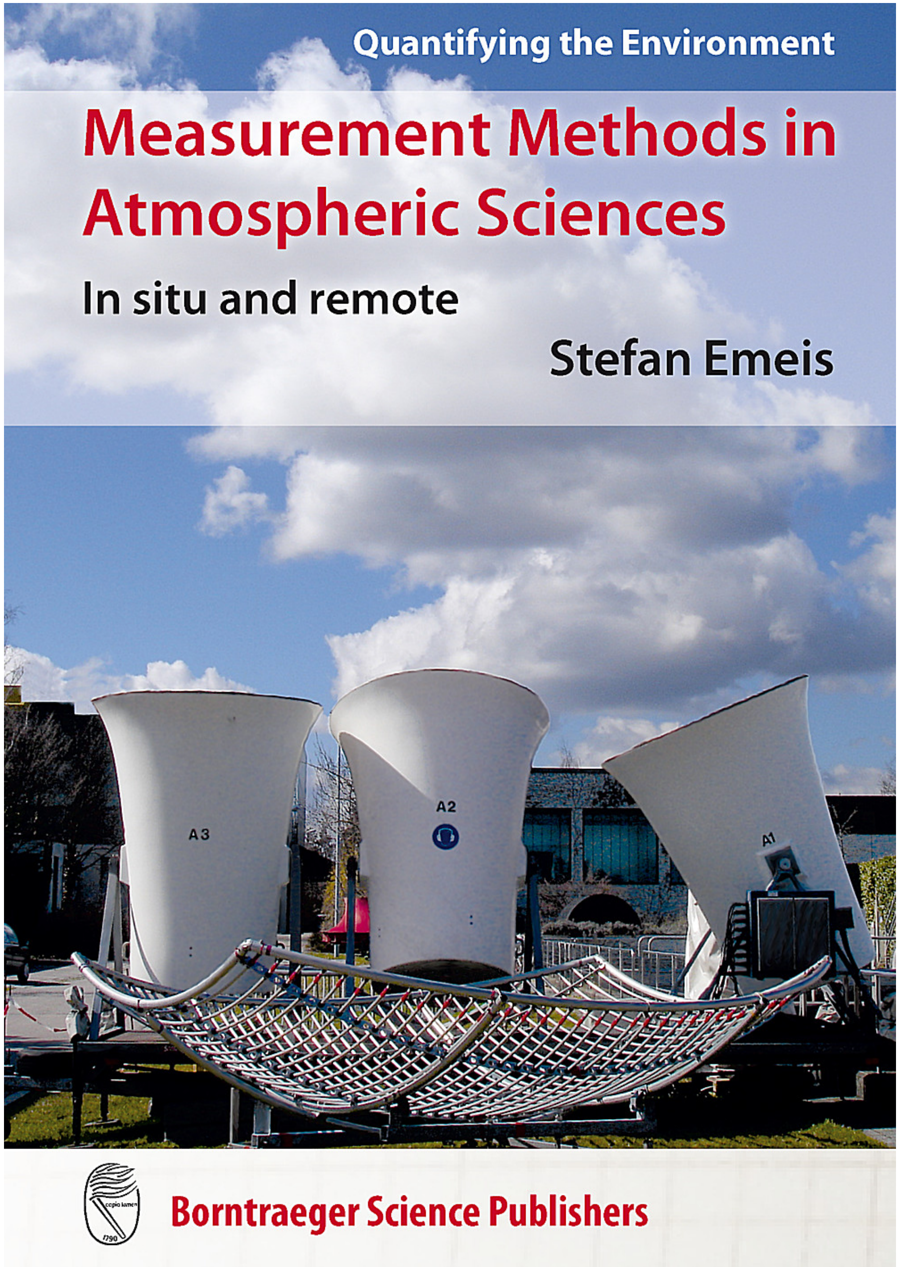
Quantifying the Environment
Measurement Methods in Atmospheric Sciences
In situ and remote
Stefan Emeis
A3
A2
A1
Borntraeger Science Publishers

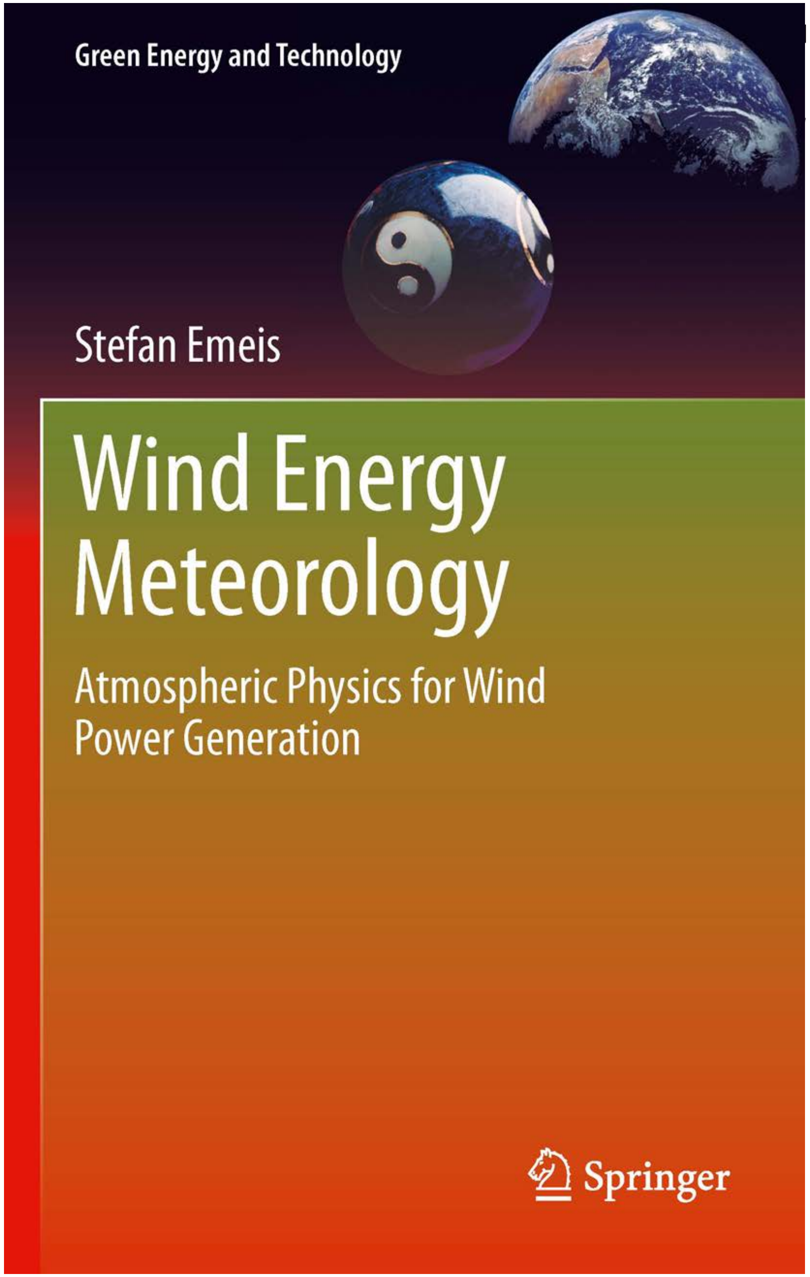
Green Energy and Technology
Stefan Emeis
Wind Energy Meteorology
Atmospheric Physics for Wind Power Generation
Springer


Karlsruhe Institute of Technology
Thank You
for your
attention